Surveys in Geophysics
https://doi.org/10.1007/s10712-026-09956-5

Present-Day Sea Level Variations in Coastal Areas from Daily to Multidecadal Time Scales: Observations and Causes

A. Cazenave[1] · R. Almar[1] · P. Almeida[2] · N. K. Ayoub[1] · J. H. Bettencourt[3] · F. Birol[1] · W. Han[4] · M. Herrmann[1] · S. Jevrejeva[5] · L. Leclercq[1] · F. Niño[1] · J. Oelsmann[6] · F. Papa[1] · S. Ponce de León[7,8] · A. Tarpanelli[9] · V. D. Vinh[10]

Received: 21 October 2025 / Accepted: 24 July 2026

Abstract
Climate-related sea level changes near the coast may deviate from what we observe in the open ocean. In effect, coastal changes result from the superposition of the global mean sea level rise, regional sea level trends, plus local contributions related to processes specific to nearshore areas. The latter operate on a broad range of timescales, from subdaily to multidecadal. They include ocean tides, atmospheric forcing, wind and waves, trapped coastal waves, coastal currents, river discharge in deltas and estuaries, natural climate modes and remote steric and mass effects. Changes in coastal ocean circulation driven by bathymetry or in coastal morphology and changing forcing factors can also impact coastal sea level. Such coastal processes not only produce coastal sea level changes, but also mediate the coastal response to open-ocean forcing. Vertical crustal motions are an additional factor causing sea level to vary with respect to the ground, in a proportion often larger than current climate-related sea level changes. Due to all involved processes, coastal sea level can significantly vary from one region to another. Here, we first discuss how coastal sea level is measured by in situ and space-based observing systems. Next, we review all processes causing sea level variations at the coast, from high-frequency extreme events to long-term multidecadal changes. We finally discuss different types of models developed for process understanding.

Keywords Sea level · Coastal sea level changes · Vertical land motions · Coastal processes · Remote sensing of coastal zones · Modeling

Article Highlights

- Coastal zones, the home of more than 10% of the world population, currently suffer multiple stresses due to natural phenomena and human activities.
- Climate related sea level rise, often amplified by ground subsidence, is one of them. Here we discuss how sea level and vertical land motions are measured at the coast.

Extended author information available on the last page of the article

Published online: 14 August 2026

- We also discuss the many phenomena that cause coastal sea level changes, from subdaily to multidecadal time scales, as well as modeling approaches developed for process understanding.

1 Introduction

Sea level is the height of the sea surface expressed either in a geocentric reference frame (called 'absolute' sea level) or with respect to the moving Earth's crust (called 'relative' sea level). Absolute sea level variations result from changes in the volume of water filling ocean basins (either due to water density or mass changes) while relative sea level variations designate sea surface height changes with respect to the ground (accounting thus for both 'absolute' sea level changes and vertical land motions/VLMs).

Sea level variations spread over a very broad spectrum. On geological time scales (~ 5–100 million years –Myr-), large amplitude (~ 100 m) of sea level changes depend primarily on tectonic processes (e.g., large-scale change in the shape of ocean basins associated with seafloor spreading and mid-ocean ridges expansion) as well as on the existence or not of polar ice sheets (Rohling et al. 2022). On 10 000–100 000-year time scales, glacial/interglacial cycles driven by changes of the Earth's orbit and obliquity also cause ~ 100 m amplitude sea level variations (PAGES 2016). On shorter time scales (100–1000 years), modest (a few meters) sea level changes occur in response to natural climate forcing factors (variations of solar irradiance and volcanic eruptions). At interannual to multidecadal time scales, natural variability inside the climate system, related to atmosphere–ocean coupling phenomena such as the El Niño-Southern Oscillation –ENSO, North Atlantic Oscillation –NAO, Pacific Decadal Oscillation- PDO (Han et al. 2019), is a major cause of sea level variations. However, since the beginning of the twentieth century, anthropogenic global warming has greatly influenced the global mean sea level through ocean warming and associated thermal expansion, as well as ocean water mass increase caused by land ice melting (Church et al. 2013). Beside causing the global mean sea level to rise by about 20 cm since the early 1900s (Dangendorf et al. 2017), human-induced global warming also influences extreme sea levels that currently increase in frequency and intensity (IPCC 2022a).

Sea level also varies at subannual and annual time scales. Significant seasonal variations affect sea level from global to local scales. In terms of global average, they are explained by the seasonal cycle of the global water cycle and of ocean temperature in response to the seasonally varying incoming solar radiation (e.g., Chen et al. 1998; Minster et al. 1999). Seasonal changes also affect coastal sea level (Barroso et al. 2024). Intraseasonal ocean sea level variations are related to basin-scale wind variability (e.g., Fu 2003). At much higher frequency, the gravitational attraction of the sun and moon causes periodic sea level oscillations, the well-known ocean astronomical tides.

As discussed by Woodworth et al. (2019), at the coast, sea level varies over a broad range of temporal scales, in response to a variety of forcing factors. These include local (often high-frequency) drivers such as astronomical tides, wave-induced setup and run up, shelf currents, storm surges caused by extreme weather events, atmospheric loading, and local changes in hydrology. These local phenomena can in some cases interact with subseasonal, seasonal, interannual and decadal variability, causing amplified sea level variations by resonance effects (Idier et al. 2019). Longer-term variations, from years to multi-decadal, due to the global mean sea level rise and regional changes also contribute to coastal sea level.

The complexity of the coastal zone arises precisely from the superposition and interaction of these different processes, which often make their combined effects more significant than if they occurred individually (Ponte et al. 2019). This complexity is of particular concern in a global context where coastal zones host dense populations, support critical ecosystems, and sustain major economic activities, making them especially relevant from a socioeconomic perspective. Consequently, understanding coastal sea-level variations, from daily to multidecadal timescales in coastal environments is essential not only for advancing scientific knowledge but also for supporting robust risk assessments and effective adaptation strategies (e.g., Nicholls 2011).

In this review we focus on local (coastal) sea level variations (but briefly discuss the global and regional scales) and on temporal scales ranging from subdaily (i.e., tides and extremes) to multidecadal timescales. We address both absolute and relative coastal sea level changes. Because of previously published reviews on coastal sea level (e.g., the collection of review articles in Ponte et al. 2019), here we focus on the most recent developments in this research domain. The paper is organized into six sections, as outlined below. Section 2 discusses how coastal sea level is measured using in situ (tide gauges) and, more recently, space-based tools (satellite altimetry,) as well as the advantages and drawbacks of each observing system. Space-based methods to measure VLMs are also presented. Section 3 provides an overview of the forcing factors acting at high frequency (astronomical and loading tides; waves; storm surges and atmospheric loading), as well as their inferred effects on sea level in terms of amplitude and area of influence. Section 4 discusses other types of climate-related forcing factors and associated mechanisms, acting at global and regional scales but influencing coastal sea level, with focus on interannual time scale (land ice melt, ocean temperature changes, glacial isostatic adjustment and fingerprints of present-day land ice melt, etc.). This section also presents the effects of climate modes on coastal sea level, as well as land-sea interactions, in particular effects of river runoff on coastal sea level. Section 5 presents models which are complementary to observations to understand the processes (global and regional circulation models; high resolution hydrodynamical coastal models, wave-current models), their ability to reproduce sea level variations in coastal areas, and also for forecasting future trajectories. A conclusion with a few recommendations is proposed in Sect. 6.

2 Measuring and Modeling Sea Level Changes and Vertical Land Motions at the Coast

Historically, sea-level measurements served practical purposes such as harbor operations and navigation. Today, with climate change exacerbating the risks of flooding and erosion, they are indispensable for ensuring the safety of coastal populations and the protection of ecosystems. This is why considerable efforts are currently being made to improve coastal sea-level observations through new instruments, enhanced processing approaches, and the integration of multiple measurement types and models (Marcos et al. 2019; Becker et al. 2020, 2024;Djeumeni et al. 2024).

The two main tools that are currently used to measure present-day sea level variations are based on in situ tide gauges and altimeter satellites. Tide gauges provide relative sea level measurements (i.e., with respect to the moving ground) while altimeter satellites measure absolute sea level in a geocentric reference system. Each of the two techniques has its own advantages and limitations. This section summarizes the current status of these two kinds of measurements as well as of space-based precise positioning techniques dedicated to measure VLMs.

2.1 Tide Gauges

Sea level measurement from tide gauge has long been used for defining the reference level for national height systems, harbor operation and safety, and aiding navigation. They provide very precise observations of sea level change in intervals ranging from a few seconds to multi-decades, at the locations where they are installed (precision <0.3 cm for modern tide gauges, Martin Miguez et al. 2012, IOC, 1985). In particular, tide gauges inform on historical sea level change along continental coastlines and islands, with some instrumental records available since the 1700s (Ekman 1988) The largest tide gauge data base of monthly and annual mean sea level records is the Permanent Service for Mean Sea Level (PSMSL, https://psmsl.org/, Holgate et al. 2013) which contains data for the twentieth century from ~ 2000 sites maintained by about 200 nations.

The records are somewhat inhomogeneous in terms of data length, geographical locations and quality. For multidecadal sea level studies, only ~ 10% of this data set is usable because of data gaps and limited tide gauge distribution in the past decades. However, it provides the historical reference of very high value to which current sea level rise can be compared. High frequency tide gauge data are also available from University of Hawaii Sea Level Centre (UHSLC, https://uhslc.soest.hawaii.edu/) and a large number of national data services. They are the primary information about extreme sea levels. Tide gauges complying with Global Sea Level Observing System (GLOSS) standards should be capable of measuring instantaneous sea level with an accuracy better than 1 cm, in all conditions of tide, waves, currents, and weather (Gobron et al. 2019, IOC, 2016).

Tide gauges measure sea level relative to the ground; consequently, other geophysical signals are also captured, e.g., VLMs. In active tectonic and volcanic regions, or in areas

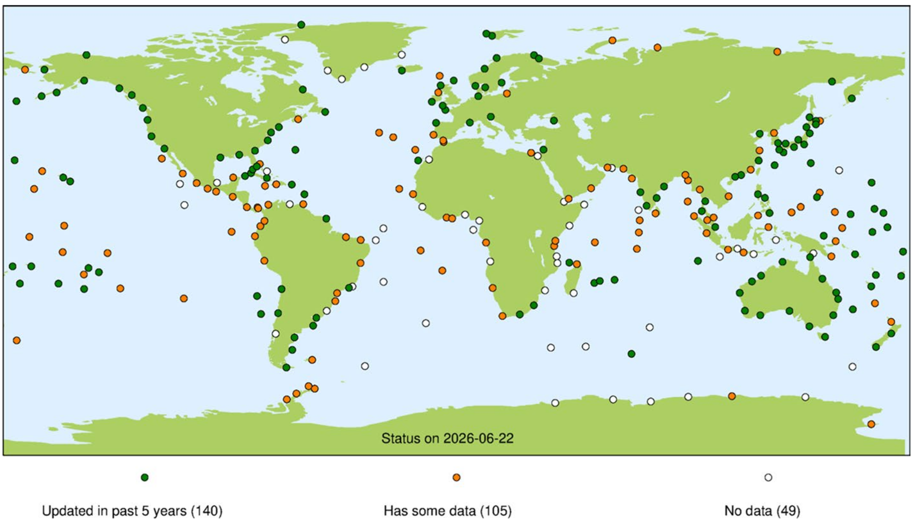

Fig. 1 Current status (June 2026) of the GLOSS core tide gauge network. No data may also mean 'not available'

subject to strong ground subsidence due to natural processes (e.g., sediment loading in river deltas) or human activities (groundwater and oil/gas extraction), tide gauge data are directly affected by the corresponding ground motions. Postglacial rebound, the visco-elastic response of the Earth's crust to last deglaciation (also called "Glacial Isostatic Adjustment/GIA"), as well as its elastic response to present-day ice sheet mass loss are other processes causing VLMs, especially in polar regions. While for comparing with climate-related sea level variations VLMs need to be removed from tide gauge records, there is no need to do so when assessing the impacts of total, relative sea level changes in coastal areas since tide gauge data directly provide this information.

Figure 1 shows the current status (June 2026) of the GLOSS core network (a global set of 290 tide gauges).

Tide gauges available since the late nineteenth century have reported significant sea level rise since the beginning of the industrial era (Jevrejeva et al. 2008; Dangendorf et al. 2017; Fox-Kemper et al. 2021). During the twentieth century, sea level rose at a mean rate of ~ 1.5 mm/yr (e.g., Frederikse et al. 2018; Palmer et al. 2021; Fox-Kemper et al. 2021) but significantly accelerated since 1960 (Dangendorf et al. 2019; Fox-Kemper et al. 2021), faster along the world coastlines than globally (Qu et al. 2023).

2.2 Satellite Altimetry

Since the early 1990s, satellite altimetry has become the complementary tool to tide gauges for measuring sea level. Satellite altimetry offers near global coverage in space, with a few days revisit time, and presently provides ~ 34 years of continuous data from different missions (Nerem et al. 2010; Legeais et al. 2018; Stammer and Cazenave 2018). As mentioned above, satellite altimetry measures 'absolute' sea level variations in a geocentric reference frame. The concept of the satellite altimetry measurement is relatively simple: the onboard radar altimeter emits microwave radiation toward the sea surface below the satellite, which is then partly reflected back to the satellite. Assuming constant propagation velocity of the wave, the measurement of the round-trip travel time readily provides the height of the satellite above the instantaneous sea surface (called 'range'). The sea surface height above a reference fixed surface (typically a conventional reference ellipsoid) is then obtained by the difference between the altitude of the satellite above the reference (deduced from precise orbitography) and the range. In practice, the estimated sea surface height has to be corrected for various factors: atmospheric effects on the radar signal, instrumental drifts, bias between successive altimetry missions, and sea state bias to remove errors due to the presence of ocean waves. Other corrections are also applied to remove unwanted geophysical signals, such as the geoid variations, barometric effects, or solid Earth, pole and ocean tides (e.g., Escudier et al. 2018). High-precision satellite altimetry started with the launch of Topex/Poseidon in 1992 followed by its successors, Jason-1, Jason-2, Jason-3, Sentinel-6 Michael Freilich and Sentinel-6B, launched in 2001, 2008, 2016, 2020 and 2025, respectively. These are considered as reference missions for long-term sea level studies due to their remarkable stability and continuity. Other satellite altimetry missions also exist, with different orbital characteristics (e.g., ERS-1,2, Envisat, SARAL/AltiKa, Sentinel 3, Cryosat-2…), leading to a greater measurement coverage of the ocean surface (Stammer and Cazenave 2018). The revisit time of the Topex/Poseidon, Jason -1,2,3 and Sentinel 6 missions is ~ 10 days. The accuracy of an individual sea surface height measurement for the classical nadir altimetry missions has now reached the 1–2 cm level (e.g., Escudier et al. 2018), allowing a precision on the global mean rate of rise of ~ 0.3 mm/

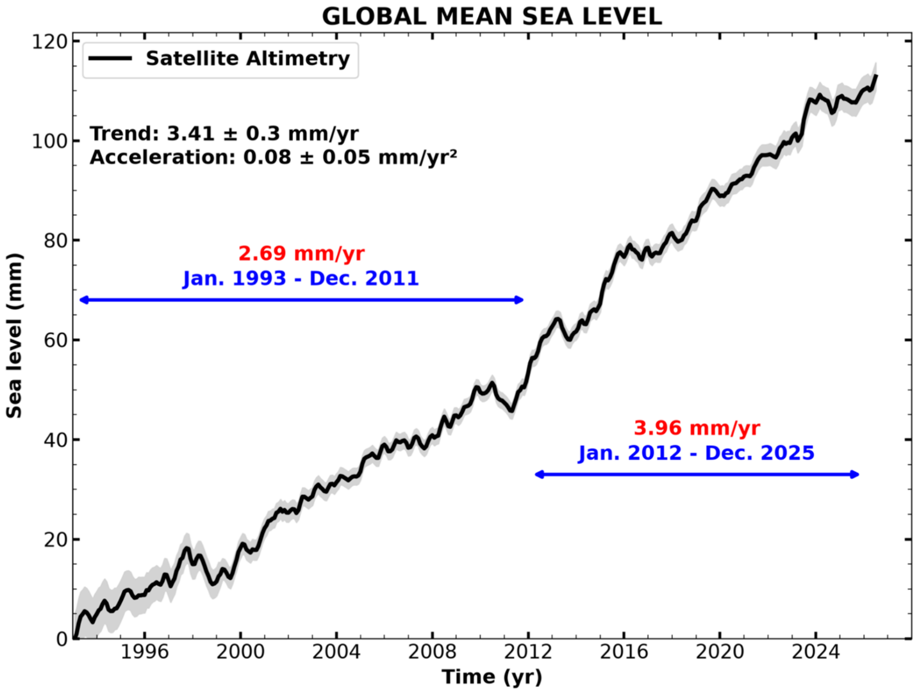

Fig. 2 Altimetry-based global mean sea level rise from January 1993 to June 2026 (black curve, seasonal signal and absolute GIA removed; Topex-A drift and Jason-3 radiometer drift corrected) and associated uncertainty (shaded area) (data from AVISO; www.aviso.fr)

yr (Ablain et al. 2019; Prandi et al. 2021). The temporal evolution of the global mean sea level from satellite altimetry since early 1993 is shown in Fig. 2. Besides a long-term sea level increase over the past 34 years (at a mean rate of 3.4 ± 0.3 mm/yr and an acceleration of ~ 0.08 ± 0.05 mm/yr^2, update of Guerou et al. 2023), temporary positive or negative anomalies of a few mm amplitude are related to ENSO events (Nerem et al. 2010). The global coverage of altimeter satellites also allows measuring long-term sea level trends variations throughout the oceanic domain (Fig. 3). While since the early 1990s, sea level has been rising almost everywhere (except in two limited regions south of Greenland and around West Antarctica), some regions (e.g., western north, central and south Pacific, southern Ocean, Indian Ocean) display higher than average sea level rise.

While satellite altimetry has become an essential tool for monitoring open ocean sea level, within 20 km from the coast, the data accuracy is degraded due to the contamination of land reflections within the radar echoes and unsuitable corrections in coastal ocean conditions (e.g., Vignudelli et al. 2019). This has resulted until recently in a total absence of validated altimetry-based sea level measurements in the world's coastal zones. Besides, since the beginning of the altimetry era, sea level measurements taken from space were based on nadir altimetry along the satellite tracks, with large gaps between the satellite tracks. However, with the launch of the SWOT (Surface Waters Ocean Topography) space mission at the end of 2022, we have entered a new era of satellite-based sea level measurements (Fu et al. 2024). SWOT embarks novel altimetry technology (a radar interferometer, Rodriguez et al. 2017), allowing 1 km resolution

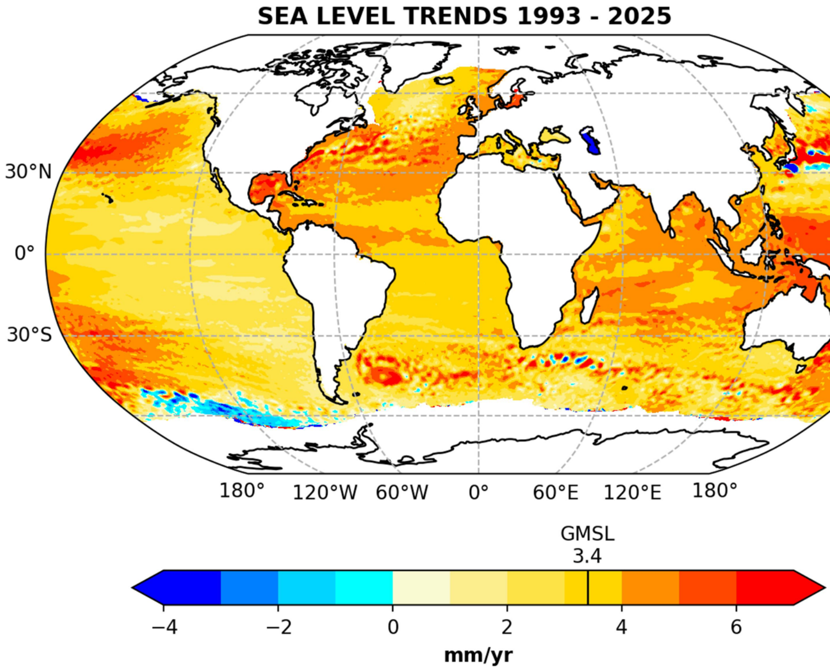

Fig. 3 Altimetry-based regional sea level trends from January 1993 to December 2025. The gridded data are from the Copernicus Climate Change Service (C3S; www.climate.copernicus.eu)

over two 50 km wide swaths on each side of the satellite track, hence providing unprecedented 2-dimensional coverage of the oceanic domain, including the coastal zones (Morrow et al. 2019). Note that over land the resolution is even higher, on the order of 100 m. Hence, SWOT provides much higher cross-track resolution and sea level measurements much closer to the coast than traditional nadir altimeters (of about 1 km compared to ~ 20 km). However, given the importance of the pre-SWOT altimetry data archive for observing and studying coastal sea level changes on the long-term, and considering that SWOT data record remains short, large efforts have been carried out in the recent years to retrieve coastal sea level estimates from it across the world's coastal zones (e.g., Passaro et al. 2014, Birol et al. 2021, Benveniste et al. 2020, Cazenave et al. 2022, Peng et al. 2025). These works have successfully produced long-term time series of coastal sea level, based on the reprocessing of high-resolution (20 Hz, i.e., 350 m) along-track altimetry data of the reference missions (namely, Jason-1, 2, 3 and Sentinel 6A) and re-estimating the altimeter range using "retracking" algorithms. So far, two global datasets on coastal sea level derived from altimetry are available. The first one has been produced in the context of the European Space Agency (ESA) Climate Change Initiative (CCI) coastal sea level project (https://climate.esa.int/en/projects/sea-level/), using the "Adaptive Leading Edge Subwaveform (ALES) retracking (Passaro et al. 2014, 2018) and improved geophysical corrections (Birol et al. 2021). The most recent version (June 2026) provides a 24-year long (2002–2025) monthly sea level dataset (time series and trends) at 1679 "virtual" coastal stations located within 8 km from the coast (update from Cazenave et al. 2022). Previous versions (coastal sea level time series over

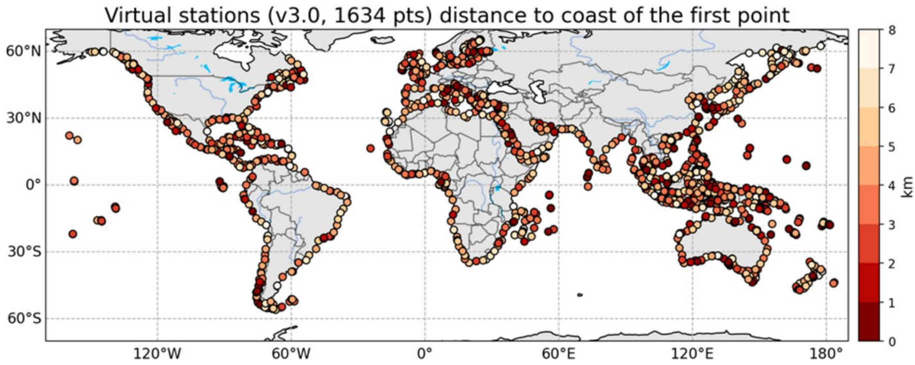

Fig. 4 Network of the 1679 coastal virtual stations located at less than 8 km from the coast (ESA CCI Coastal Sea Level project; latest version from June 2026 covering the 2002–2025 time span)

2002–2021 at 1639 virtual stations) are publicly available from the SEANOE web site (https://doi.org/10.17882/74354).

The second coastal sea level product (called IAS2024, Peng et al. 2025) uses the data from the Jason-1, 2 and 3 altimetry missions and combines different retrackers depending on the characteristics of the radar waveform (Peng et al. 2023). The latter dataset also provides along-track sea level time series since 2002 at ~ 1600 virtual coastal stations. It is publicly available at https://doi.org/10.5281/zenodo.1320805.

These coastal altimetry virtual stations usefully complement the current tide gauge network (Fig. 4). An example of coastal sea level product from the ESA CCI coastal sea level project is shown in Fig. 5. It shows estimates of sea level trends along a satellite track, from 20 km offshore to the coast (resolution of 350 m), as well as the sea level time series close to the coast over 2002–2025.

Figure 6 shows a few examples of altimetry-based coastal sea level time series at some virtual stations on which are superimposed nearby tide gauge–based sea level measurements. Good consistency between the two types of sea level measurements is observed at most sites. What the figure also shows is that when a tide gauge record suffers temporal data gaps (i.e., Seychelles Islands), the altimetry-based time series usefully completes the tide gauge records, not to mention the many sites where no tide gauge data are available (see Fig. 1).

2.3 GNSS and InSAR Techniques for Measuring Vertical Land Motions

Space-based precise positioning techniques such as GNSS (Global Navigation Satellite System) and InSAR (Interferometric Synthetic Aperture Radar) have been steadily developed and improved over the last decades to measure VLMs (Sanli and Blewitt 2001; Wöppelmann et al. 2007; Hammond et al. 2021; Shirzaei et al. 2021). GNSS measurements represent point measurements of station velocities within a geodetic reference frame and are therefore comparable to satellite altimetry observations obtained within the same reference frame. To estimate VLM rates, different modelings, corrections and time series parametrizations (i.e., detection of trends, periodic signal and offsets) have to be applied (e.g., Blewitt et al. 2016; Gravelle et al. 2023). GNSS measurements are among the most accurate and precise VLM measurements. Wöppelmann and Marcos (2016) reported relatively

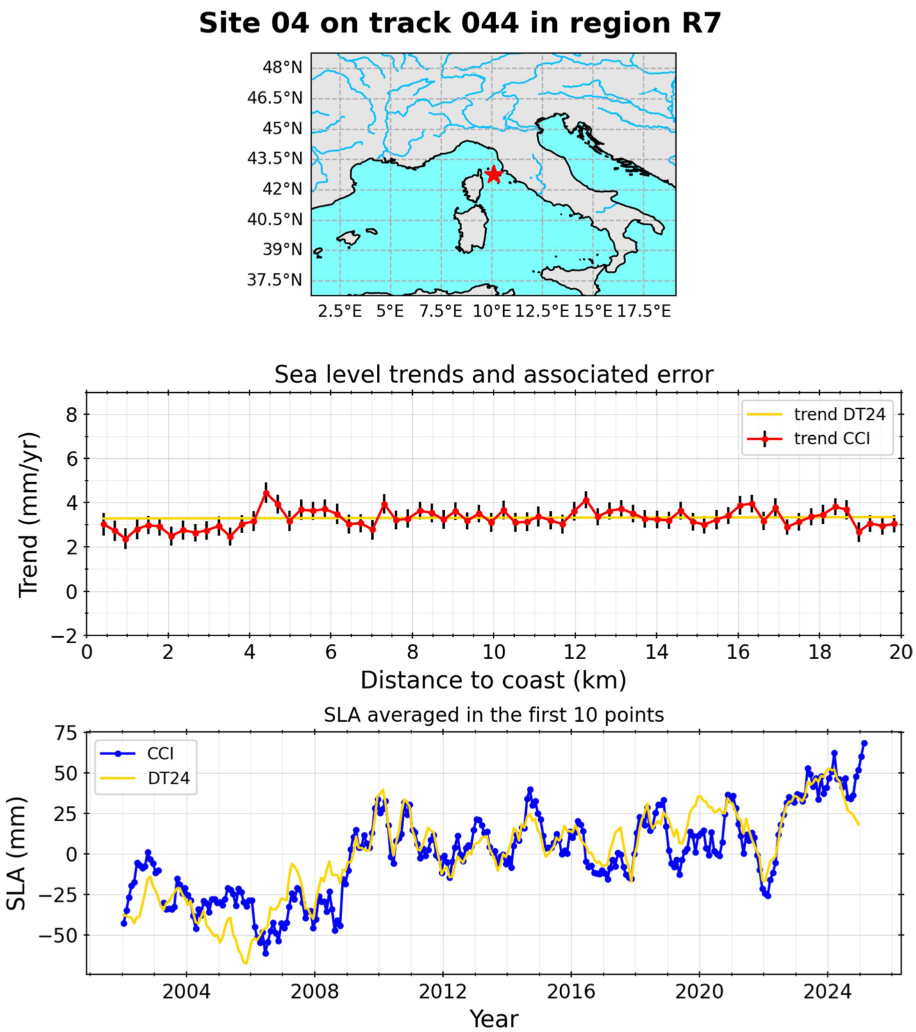

Fig. 5 Example of coastal sea level product from the ESA CCI Coastal sea level project: location of the virtual station -here the Elbe Island in the Mediterranean Sea- (top panel); Along-track sea level trends and associated errors from 20 km offshore to the coast (middle panel); Sea level anomaly (SLA) time series based on averaging data from the 10 closest points to the coast (lower panel). In the middle and lower panels, data from gridded DT2024 sea level product (https://climate.copernicus.eu/climate-indicators/sea-level) are superimposed (yellow curves)

low formal errors for GNSS–VLM rates (0.21 mm/year) when accounting for auto-correlation. Similarly, Santamaría-Gómez et al. (2012) estimated an accuracy of 0.6 mm/year for GNSS-based vertical land motion, based on at least three years of continuous data, by comparing 36 globally distributed co-located GNSS velocity estimates. Due to this high accuracy, vertical GNSS velocities serve as crucial benchmark estimates for various sea-level applications, such as GIA-model evaluation and local VLM corrections of tide gauge records (Sánchez and Bosch 2009; Sanli and Blewitt 2001).

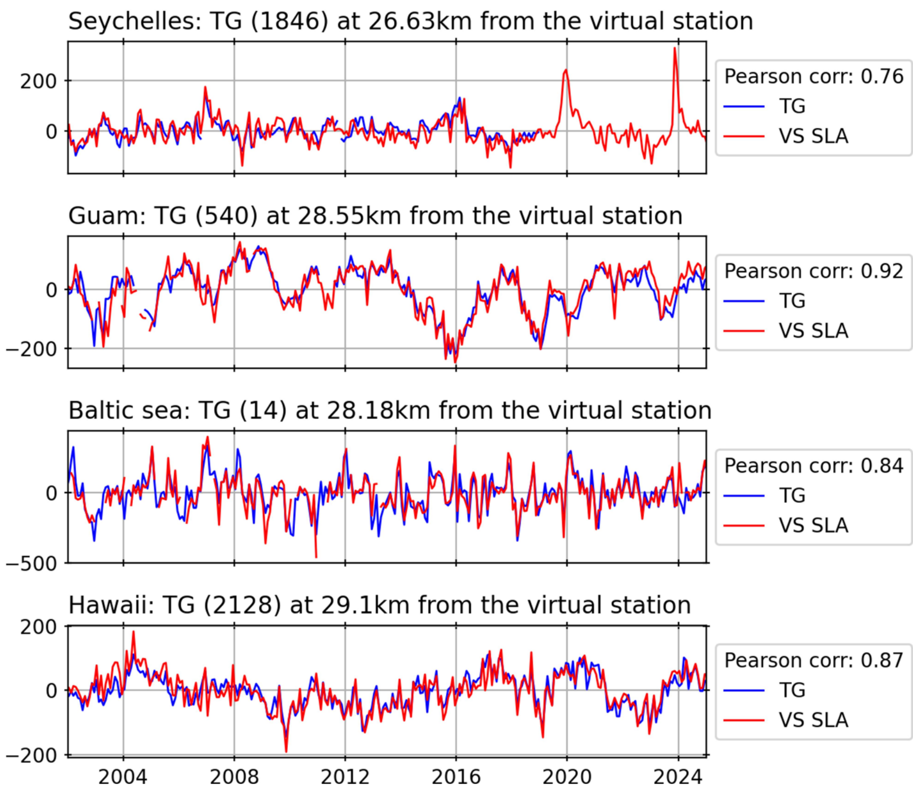

Fig. 6 Examples of 'absolute' coastal sea level time series over 2002–2025 at a few virtual stations (called vs. SLA on the figure, in red; from top to bottom: Seychelles Island, Indian Ocean; Guam, Pacific Ocean, Baltic Sea; Hawaii, Pacific Ocean), based on the latest version (June 2026) of the altimetry-based coastal sea level product (ESA CCI Coastal sea level project). Sea level records at nearby tide gauge (TG) sites are superimposed (in blue). The time series are deseasonalized and detrended. The correlation between the two time series is indicated

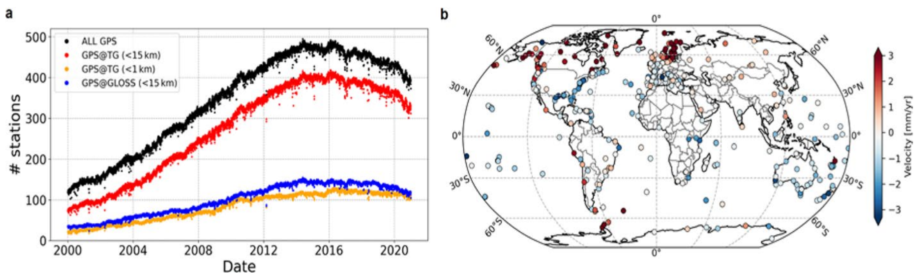

Fig. 7 **a** The evolution of station availability in ULR (University of La Rochelle)–repro3 (black) within a 15 or 1 km distance of a tide gauge (red and orange respectively) and within 15 km of a GLOSS tide gauge site (blue). **b** Vertical velocities in mm/year. (Adapted from Gravelle et al. 2023)

Different analysis centers have dedicated efforts to provide globally consistent GNSS solutions. For example, SONEL (Système d'Observation du Niveau des Eaux Littorales) is a GNSS data assembly centre for the Global Sea Level Observing System (GLOSS) and provides quality-checked VLM data from different providers at PSMSL tide gauges. Figure 7 exemplifies the availability of GNSS stations (of the ULR/University of La Rochelle—repro3 solution, Gravelle et al. 2023) in (a), and the associated velocities in (b). As can be seen, ongoing challenges are that most of the GNSS estimates are only available after the year 2000, and the availability has already started to decline after 2016. In addition, a minority of tide gauges have GNSS in close vicinity. While 457 GNSS stations are within 15 km of a tide gauge, only 135 stations are within 1 km of the tide gauge. This still highlights existing measurement gaps, and has motivated alternative approaches to estimate VLM at tide gauges (e.g. Woppelmann and Marcos 2016; Kleinherenbrink et al. 2018), or to interpolate large networks of GNSS data, e.g., from the Nevada Geodetic Laboratory, which provides more than 20,000 estimates worldwide (Blewitt et al. 2016; Hammond et al. 2021).

Although GNSS measurements are highly accurate, a major limitation is that they cannot resolve small scale VLM variability on scales from m to kms. Therefore, the InSAR technique has been increasingly utilized to determine spatially resolved VLM (~ 250 m resolution), and was already coined as "the gold standard of VLM measurements" (Ohenhen et al. 2024). InSAR estimates the line-of-sight velocities, based on the phase difference of backscattered radar signals between two SAR images taken at different time steps (e.g., Shirzaei et al. 2021). The processing of InSAR data requires several external information, e.g., of atmospheric conditions, which can influence the coherence between two SAR images, i.e. the precision of the phase observations. The phase coherence is also reduced over densely vegetated areas, which makes the estimation over these dynamic coastal landscapes challenging (Törnqvist and Blum 2024). In order to obtain VLM rates in a geodetic reference frame, the line-of-sight (LOS) velocities (which are influenced by both, vertical and horizontal motions) have to be transformed into the horizontal and vertical

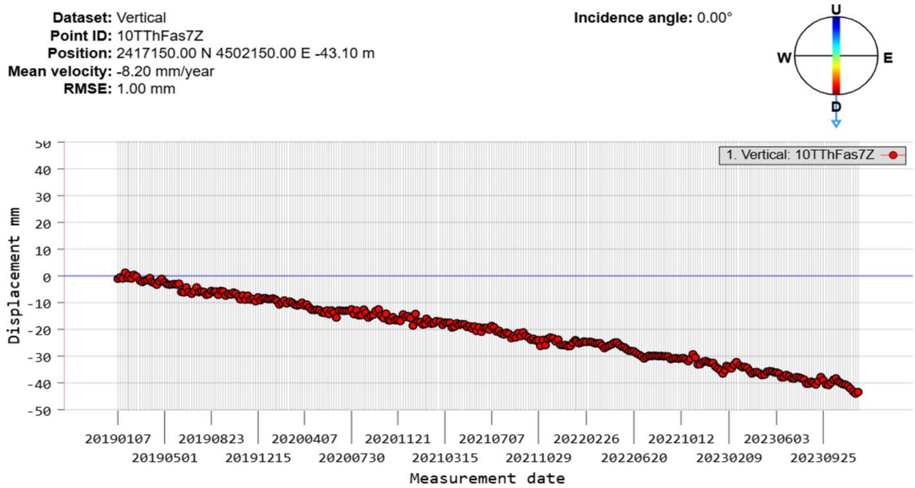

Fig. 8 Ground subsidence between 2019 and 2023 at the Po River delta based on InSAR data from the Sentinel 1 satellite. The figure shows the subsidence curve in mm at location 24.17°N, 45.02°E (*Source*: Copernicus Ground Motion Service; https://egms.land.copernicus.eu/)

components, which however requires GNSS stations with known velocities (Shirzaei et al. 2021).

Figure 8 shows ground subsidence between 2019 and 2023 at the Po River Delta in the Adriatic Sea, based on InSAR data from the ESA Sentinel 1 satellite (data from the European Ground Motion Service that provides InSAR-based VLMs over the whole Europe with a horizontal resolution of ~ 100 m; Thieblemont et al. 2024). In the example shown in Fig. 8, the subsidence rate is high and amounts to 8.2 mm/yr over 2019–2023.

It is worth mentioning that at several locations ground subsidence leads to relative sea level rise several times larger than absolute (climate-related) sea level rise (Oelsmann et al. 2026; Seeger and Minderhoud 2026), as shown by the example in Fig. 8. In the majority of cases, ground subsidence results from groundwater extraction for agriculture, domestic use and industries, as well as sediment loading in river estuaries (e.g., Minderhoud et al. 2017).

Very recently, different InSAR products have been released that cover almost the entire US coast (Ohenhen et al. 2024), Europe (Thieblemont et al. 2024), New Zealand (Naish et al. 2022), and China (Ao et al. 2024). These datasets have been employed to refine spatial information of flood risk, and to shed light on the underlying processes of human-induced or natural subsidence, which often cannot be resolved with the GNSS network alone. InSAR rates that have been transformed into VLM rates using GNSS data usually have an accuracy in the order of 1–2 mm/year. However, special caution is advised when such reference stations are not available as this decreases the interpretability of the derived rates. Other error sources are imperfect post-processing or when the reflector movement does not exactly align with land surface movement (Minderhoud et al. 2025). It should also be highlighted that InSAR measures surface elevation changes, which may sometimes differ from GNSS rates when shallow subsidence is present and not captured by the GNSS antenna due to its deep anchor depth. In summary, while InSAR has the potential to revolutionize VLM estimates and process understanding, it still 'poses risks of oversimplification and misinterpretation, especially when linked to sea-level change' (Minderhoud et al. 2025).

2.4 Advances in Estimating Glacial Isostatic Adjustment (GIA) and Gravitational, Rotational, and Deformational (GRD) Effects

GNSS, InSAR, and tide-gauge measurements are influenced by a range of VLM processes that cannot yet be fully disentangled into their individual components at the global scale. This limitation is largely due to the scarcity of in situ observations and the lack of process-based models capable of representing the full spectrum of VLM drivers (e.g., tectonic processes, shallow compaction, subsurface fluid extraction, etc.). One notable exception is the contribution from large-scale gravitational, rotational, and deformational effects associated with changes in Earth's ice history and contemporary mass redistribution. Contemporary mass loading also introduces nonlinear and spatially variable deformation into GNSS records. Understanding these effects is necessary to extrapolate trends derived from modern VLM measurements into the past and future (e.g., Frederikse et al. 2019; Dangendorf et al. 2026). Frederikse et al. (2019) showed that this deformation can reach approximately 1 mm/yr or more at many stations and may even change sign between different time spans. Consequently, linear trends derived from short GNSS records should not automatically be extrapolated over multidecadal tide-gauge records. Moreover, GNSS- and altimetry-minus-tide-gauge VLM estimates may differ because the instruments do not sample exactly the same time period. Hence, accounting for elastic deformation due to present-day mass redistribution improves their agreement (Kleinherenbrink et al. 2018; Oelsmann et al. 2022).

Where neither GNSS nor InSAR measurements are available to estimate VLM at the coast, most investigators often consider model-based GIA estimates. GIA is the

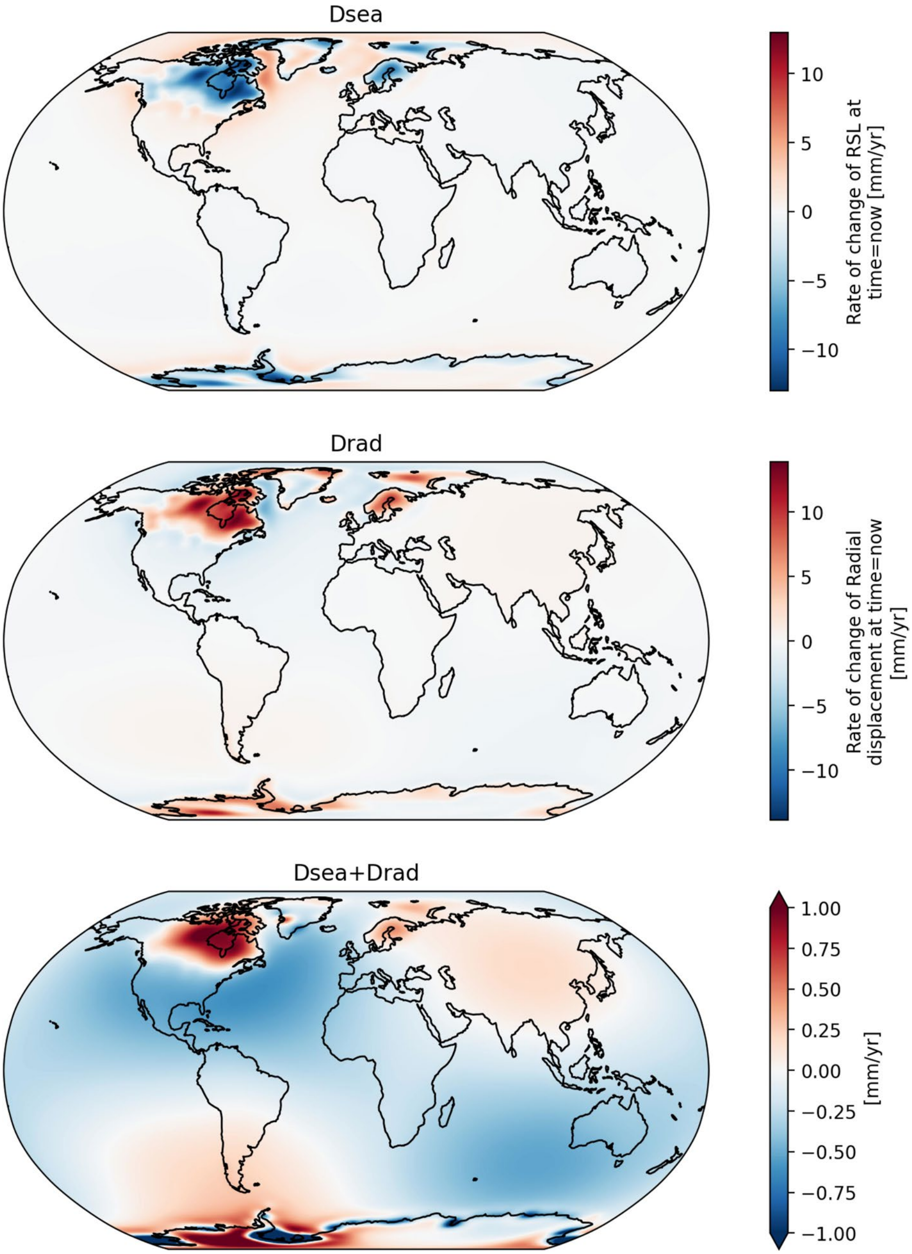

Fig. 9 GIA trend patterns for relative sea level (Dsea), vertical crustal deformations (Drad) and absolute sea level (Dsea + Drad). The maps are based on the ICE6G model of Peltier (2004)

response of the solid Earth to last deglaciation. It depends on Earth's mantle viscosity and deglaciation history (Whitehouse 2018; Spada 2017). Associated mass redistributions induce changes in Earth Gravity, Earth Rotation and visco-elastic solid Earth Deformation, commonly called GRD effects (Mitrovica et al. 2001; Milne et al. 2009; Gregory et al. 2019). This phenomenon (essentially known from modeling) gives rise to complex regional patterns in sea level change: sea level drop in the immediate vicinity of the melting bodies but sea level rise in the far field (e.g., along the northeast coast of America). GIA effects on sea level are estimated by solving the sea level equation (e.g. Farrell and Clark 1976; Mitrovica and Milne 2003 Peltier 2004). Although being a long-term process, it still impacts contemporary sea level observations. In altimetry data (i.e., absolute sea level), GIA is a small signal in terms of global average (~ -0.3 mm/yr, Peltier 2004; Tamisiea 2011; Caron et al. 2018). Its regional signature is mostly uniform, except in formerly glaciated high-latitude regions. The relative sea level signature of GIA is significantly larger. It is that quantity that needs to be considered for correcting tide gauge data from the GIA signal. In some coastal regions (i.e., along the coasts of North America), the GIA signal can reach up to 4 mm/year.

Figure 9 shows GIA trend patterns for relative sea level (Dsea), vertical crustal deformations (Drad) and absolute sea level (Dsea + Drad).

The above quoted GIA models assume radially symmetric mantle viscosity structure. However, the Earth's rheology varies strongly from place to place, affecting how it rebounds after ice melts, hence affecting GIA models. A 3D GIA model has been recently developed considering 3D viscosity fields derived from tomography and two commonly used ice-loading histories (Hightower et al. 2026). This model significantly differs from traditional GIA models in many regions. Ocean mass patterns in particular exhibit large and spatially coherent changes, especially in the Northeast Atlantic.

Contemporary changes in land ice and terrestrial water storage also generate GRD responses (Adhikari et al. 2019; Frederikse et al. 2019; Camargo et al. 2022). When mass is transferred from glaciers, ice sheets, or land–water reservoirs to the ocean, the resulting changes in Earth's gravity field, rotation, and elastic deformation of the solid Earth redistribute seawater and produce spatially varying sea-level fingerprints. Since 2002, the underlying mass changes have been observed by the Gravity Recovery and Climate Experiment (GRACE) and, subsequently, GRACE Follow-On missions, which infer monthly variations in Earth's gravity field and thereby provide estimates of mass redistribution within the cryosphere, hydrosphere, and oceans (Tapley et al. 2004, 2019; Adhikari et al. 2019). GRACE data are commonly provided as spherical-harmonic solutions or as mass-concentration, or mascon, products; the latter estimate monthly mass anomalies within predefined spatial elements and can reduce correlated errors and land–ocean leakage, although their effective resolution, regularization, coastal treatment, low-degree corrections, and removal of the GIA signal remain important sources of uncertainty (Watkins et al. 2015; Save et al. 2016; Wiese et al. 2016). Estimates of the resulting GRD contribution have become crucial to determine associated (non) linear deformation patterns, as well as to regionalize the sea-level budget.

3 High-Frequency Forcing Factors on Coastal Sea Level: Processes and Observations

In this section we discuss phenomena causing high-frequency (from subdaily to monthly time scales) sea level variations at the coast. These include tides, extreme events, waves, local winds and atmospheric loading. The section concludes with a discussion of the impacts of tides and waves on coastal bathymetry.

3.1 Astronomical Tides

A major process in sea level variability is gravitational tides which act on both the solid Earth and ocean, therefore impacting both the absolute and relative sea levels. In this section, we deal with oceanic tides only, omitting vertical land motion due to astronomical gravitational forces, loading and self-attraction effects. Gravitational tides can be divided into three main species: semi-diurnal, diurnal and long period (periods from several days to several years). A permanent tide also exists. To simplify, tides propagate from the deep ocean to shelf seas (depths $< \sim 200$ m) where they dissipate due to the bottom friction (Lyard and Le Provost 1997; Pugh and Woodworth 2014). Far from the coast, dissipation also occurs through the generation of internal tides which represents about 25–30% of the total dissipation of tides (Egbert and Ray 2000). When tides reach the shelf, their amplitude increases as a result from the energy conservation principle and from local resonance when the forced tidal oscillations are close to their natural period (Pugh and Woodworth 2014). Tides on the shelf are not only amplified, but are also more complex, as the nonlinearities of the dynamics, due to advection and bottom friction mainly, lead to the generation of compound tides. In very shallow waters where the tidal elevation and the total water depth become comparable, a dependence of the tidal wave celerity on the tidal amplitude is introduced, which results in a distortion of the tidal signal (e.g., Dronkers 1986). In estuaries, interactions with the river flow can reflect in large variations of tidal amplitude between flood and low-water conditions.

When studying the decadal and climatic variations of relative sea level, one difficulty is to disentangle the low-frequency tidal signal from other oceanic slowly varying signals in long time series of sea level observations. In particular, the precession of the Moon's axis of rotation leads to the so-called nodal tide at a period of 18.61 years and to a modulation of the semi-diurnal and diurnal tides at the same period (Pugh and Woodworth 2014). How they influence the coastal sea level is quite subtle. Bult et al. (2024) show for instance, that the 18.61-year sea level variations observed at tide gauges in the North East Atlantic are due to a combination of the nodal tide and of steric sea level change resulting from the nodal modulation of the semi-diurnal tides hence of the tidal mixing.

Extreme tides also experience modulation at diverse time scales, for instance at 18.61 and 4.4-year periods (e.g. Haigh et al. 2011; Ray and Merrifield 2019). As underlined by Peng et al. (2019), the coincidence of large meteorologically induced surges and large or moderate tides can lead to disastrous flooding events. Understanding and predicting the underlying mechanisms of the impact of low frequency tidal variations on high tides as well as their interactions with storm surges is a major challenge to better assess and mitigate coastal submersion and flooding hazards. For instance, Peng et al. (2019) examine the contribution of the 18.61-year lunar nodal cycle to sea level observations from more than 570 tide gauges worldwide with the aim to predict periods of enhanced risks of flooding. In particular, they show that the 18.61-year variability of high tidal levels will be 'substantially larger than global mean sea-level rise in the next few years to decades' in several places worldwide.

Understanding and predicting the impact of long period tides on sea level implies to understand how tides respond to climatic forcing and to global changes. Ray (2022) discusses the variability of M_2 tides at seasonal time scales. Haigh et al. (2019) provide an extensive review of studies on changes of tides from paleo-timescales to decadal scales in the 20th and early twenty-first centuries and on projections over the twenty-first century and beyond. They first note that the largest low-frequency changes in tidal properties occur in estuaries. Changes in bathymetry and channels geometry due to human activities (dredging, riverbank development, etc.) are the primary factors there, followed by changes in vertical mixing and dissipation, mainly controlled by flow-induced bottom friction, stratification, bed roughness, sediment concentration, and by changes in river discharge both at seasonal and interannual to climatic time scales (see also the review of Talke and Jay 2020). At the shelf and in the global ocean, many factors can impact the amplitude of tides. Changes in water depth (due for instance to sea level rise or to tectonic activities), shoreline position, sea ice extent and seabed roughness alter resonance, the propagation speed of tidal wave, the strength of frictional effects both at the surface and at the bottom and the location where dissipation occurs (Haigh et al. 2019). Changes in stratification impact both the viscosity in the water column hence the tidal currents and elevation (e.g., Muller et al. 2014) and the conversion to internal tides (e.g., Opel et al. 2024). Interannual variations of spatial distribution of water level, depending on the low-frequency sea-level pressure patterns, can impact the propagation of the tide, as suggested for instance by Pineau-Guillou et al. (2021) in the North Atlantic under the effect of NAO variability.

Over the past two decades, numerous studies have examined tidal projections in the context of future climate, taking into account various factors (average sea-level rise, increased stratification, changes in ice cover, and the position of coastlines). Haigh et al. (2019) show that it is not easy to draw a general conclusion from these studies. They suggest however that sea level rise is more likely to impact tides in resonant or near-resonant basins (such as the North Atlantic) where tidal dissipation is sensitive to the extent of dried/flooded shelf seas.

All these processes are mostly investigated through global, regional or coastal numerical simulations either in realistic configurations or through dedicated sensitivity studies. Because of the complexity of the processes involved and their interactions, further research is needed, in particular based on observations to better understand the past changes and to better calibrate and assess the models. Thanks to the precision of the measurements and data processing, the multi-decade nadir altimetry datasets are extremely valuable tools. Thanks to advances in coastal altimetry (reprocessing of nadir satellite sea-level time series using appropriate algorithms; see Sect. 2.2), it is now possible to derive new tidal observations up to a few kilometers from the coast (Djeumeni et al. 2024; Seifi and Filmer 2023). The combination with the novel SWOT observations that allow to explore the 2D variations of sea level at high resolution, notably in coastal and estuarine regions, paves the way for new insights into the mechanisms of tidal propagation and dissipation.

3.2 Extreme Sea Levels Due to Meteorological Effects (Storm Surges, Atmospheric Loading)

Extreme sea level events are short-lived (lasting from hours to days) and consist of exceptionally high or low local sea surface heights. They are usually driven by the interaction of

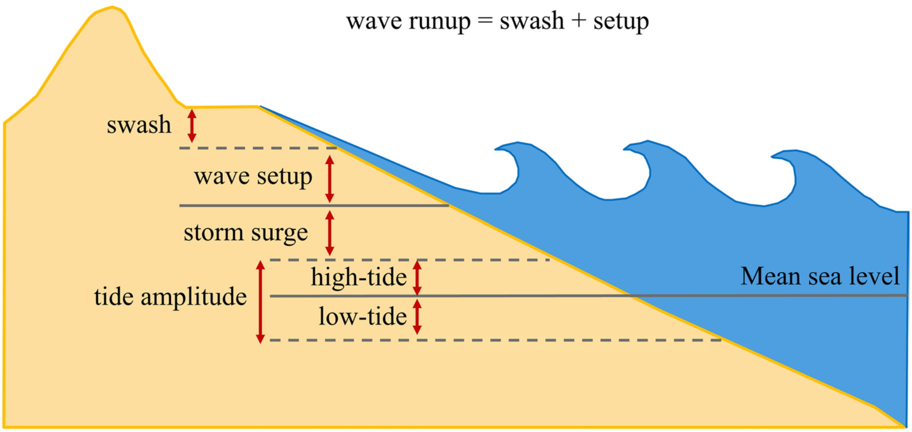

Fig. 10 Schematic representation of the different contributions to extreme sea levels near the coast

multiple oceanic and atmospheric processes operating across a wide range of timescales (from hours to decades and beyond), including tides, storm surges, waves, seasonal to interannual background sea-level anomalies, and river discharge (see Sects. 4.2 and 4.4), with their relative importance varying across different coastal settings (Berghuijs et al. 2019). Event-scale extremes typically arise from changes in local mean sea level in combination with storm surges, waves, and astronomical tides (Fig. 10), with storm surges and waves being primarily driven by meteorological conditions, e.g. changes in atmospheric pressure (i.e., loading) and wind associated with propagation of tropical and extratropical cyclones, their intensity, moving speed and path. The magnitude and frequency of extreme sea levels near the coast are strongly modulated by local conditions such as water depth, shelf width, bathymetry and river runoff, which affect wave, tidal and storm surge dynamics, and their interactions (De Dominicis et al. 2020; Idier et al. 2019). The magnitude of storm surges can be amplified with sea level rise due to the decreased effect of bottom friction (Liu and Huang 2019) or diminish due to the reduction of the surface wind stress on the water column (De Dominicis et al. 2020). As illustrated in Fig. 10, ocean waves breaking on the shore amplify the magnitude of extreme sea levels at the coastal location due to: (1) changes in wave setup, (2) the temporary increase in mean water level, caused by the momentum of breaking waves at some distance away from the shore; and (3) wave run-up, the maximum vertical elevation reached by the wave breakup and its uprush to the beach (Melet et al. 2018).

The duration of extreme sea levels can vary significantly due to numerous physical mechanisms contributing to the extreme event, typically lasting from a few hours to several days. The exact length depends on factors such as the storm's strength and size, its speed and path, the shape of the coastline, waves and local tidal forces. The magnitude of observed extreme sea levels is highly variable, with one of the greatest recorded storm surges being generated by Hurricane Katrina (August 2005), which produced extreme sea level of more than 8 m (FEMA 2006).

The representation of different processes, e.g. separation of the local (e.g., wave setup near the coast) from large-scale ocean processes (e.g. surges and tides) is the major challenge to interpret tide gauge-based sea level observations. In addition, the effects of waves and river flow are typically not well captured by tide gauges due to their installation in sheltered areas (e.g., Hoeke et al. 2013). There are limited studies aiming to separate the local from large-scale forcings on extreme events using tide gauge records. For breakdown of the local and large-scale processes controlling the exceptional Venice floods of November 2019, the tide gauge time series was decomposed to identify the components associated with different atmospheric processes, based on their time–frequency range, in addition to the separation of tidal and non-tidal components (Ferrarin et al. 2021). Oceanic and meteorological conditions (observed and modeled) during storm Xaver (2013) in the German Bight were analyzed by Dangendorf et al. (2016), providing a breakdown of the components of tide gauge records.

3.3 Waves

On wave-exposed coasts, waves play a fundamental role in sea-level variability and extremes, as they contribute directly to total water levels through wave setup and wave run-up. The run-up height is defined as the maximum vertical excursion of the water above the still water level induced by waves. It is commonly decomposed into two components: a quasi-steady increase in mean water level, the wave setup, generated by the cross-shore radiation stress of breaking waves, and an oscillatory component, the swash. The swash itself comprises two distinct phases: an upslope, landward-directed flow, usually referred to as the uprush, and a downslope, seaward-directed flow, commonly known as the backwash (Dean and Dalrymple 1984). The magnitude of wave run-up is controlled by a number of physical factors, primarily related to the offshore wave conditions and the coastal morphology. Offshore wave height and period are key drivers, as larger and long-period waves tend to induce greater run-up (Holman 1986a, b; Stockdon et al. 2006a, b). The wave spectrum, including its directional spreading, also influences run-up by modulating the distribution of incident wave energy alongshore. The coastal morphology, including the beach slope and nearshore bathymetry plays a central role, with steeper and more reflective beaches favoring higher run-up excursions compared to dissipative, low-sloping profiles (Wright and Short 1984a, b). Sediment characteristics such as texture can further modify run-up by altering energy dissipation and swash dynamics. For example, on coarse-grained beaches, which are common in higher latitudes, the larger sediment size enhances hydraulic conductivity (infiltration) and increases frictional resistance to uprush and backwash, thereby significantly modifying run-up behavior relative to sandy beaches (Masselink and Russell 2013). The presence of infragravity waves, generated by groups of breaking waves, has also been shown to significantly enhance run-up variability at low frequencies, especially on dissipative beaches (Guza and Feddersen 2012a, b). Overall, run-up emerges from the complex interplay among offshore wave forcing, nearshore hydrodynamics, and coastal morphology, making it highly site-specific and challenging to predict. Observing run-up directly is particularly challenging due to the mobility of the waterline and the fine spatial and temporal resolution required, which makes in situ instrumentation logistically complex and often impractical. Recent advances include the use of remote sensing techniques such as LiDAR to capture run-up dynamics with high accuracy (Almeida et al. 2015). In practice, however, most recent global assessment studies rely on empirical parameterizations (e.g., Stockdon et al. 2006a, b), while regional to local investigations increasingly employ high-resolution process-based models such as SWASH or Xbeach (Roelvink et al. 2009), despite their considerable computational demand. Previous studies have demonstrated the significance of wave run-up for coastal total water level variability and extremes. Melet et al. (2018) showed that interannual-to-decadal changes in wave setup and swash, driven by offshore wave climate variability, can be of comparable magnitude to steric and land-ice contributions at the coast. At longer timescales, global projections suggest that average changes in wave setup will remain modest, yet at regional scales they may still represent a non-negligible contribution to coastal deviations from mean sea-level rise (Melet et al. 2020a,b). Reviews by Dodet et al. (2019) emphasize that wave-driven contributions span a broad frequency range, from seconds to hours for run-up processes to multi-annual fluctuations linked to wave climate variability. The role of run-up becomes particularly critical under climate change: small increases in mean sea level (10–20 cm) have already been shown to double coastal flooding frequency in the tropics (Vitousek et al. 2017), and projections indicate very likely increases in 100-year extreme water levels of 58–172 cm by 2100 under high-emission scenarios, partly due to wave contributions (Vousdoukas et al. 2018). Almar et al. (2021) further estimated that overtopping hours driven by the combined action of tides, surge, and run-up have already increased by nearly 50% over recent decades, with projections indicating up to a 50-fold increase by the end of the century. Waves also play a critical role in compound flooding, interacting with tides, storm surges, river discharge, or extreme rainfall, and generating highly nonlinear responses (Hao et al. 2018; Wahl and Chambers 2015; Bevacqua et al. 2019). These compound processes, highlighted by the IPCC SROCC (IPCC 2019) as a major source of uncertainty (Collins et al. 2019), are particularly important in estuarine and deltaic systems where morphology and hydrology interact. Improving the representation of wave contributions to extreme sea levels, through enhanced observations, advanced process-based modeling, and their integration into risk assessments, remains a critical challenge for predicting coastal hazards.

3.4 Local Winds and Atmospheric Loading and Coastal Trapped Waves

At sub-daily to monthly timescales, surface winds and atmospheric loading are the dominant forcing factors for coastal sea level variability, including the wind waves and storm surges discussed above (see review by Woodworth et al. 2019 and references therein). Atmospheric loading operates via the Inverse Barometer (IB) effect, where a 1 mbar increase or decrease in sea-level pressure lowers or raises the sea level by approximately 1 cm. At subinertial frequencies with periods of days and longer, local longshore winds over the shelf can induce coastal Ekman mass divergence (convergence), resulting in coastal upwelling (downwelling) and a corresponding local decrease (increase) in coastal sea level. These local sea-level anomalies, generated by longshore winds and/or IB effects, can also influence coastal sea level in remote regions through the propagation of coastal trapped waves (CTWs), which travel with the coast on their right (left) in the Northern (Southern) Hemisphere (see the review by Hughes et al. 2019, and references therein).

Recent studies suggest that along shelf wind stress, together with CTWs, is a dominant driver of coastal dynamic sea level variability at daily to yearly timescales in the Mid-Atlantic Bight during 1982–2021 (Lentz 2024); and area-averaged onshore/offshore winds, which drive water toward or away from the coast, can play an important role in affecting coastal sea level in some regions of the U.S. Atlantic and Gulf coasts over the 2000–2021 period (Kataraihya and Wdowinski 2026). Studies based on numerical model simulations and gridded satellite altimetry sea level data show that, at subseasonal timescales, coastal longshore winds make a significant contribution to extreme sea level events along the Indonesian coast (Kamp et al. 2024), while CTWs driven by equatorial winds explain about

70% of the sea level variability in a 0.5° wide coastal band along the African coast in the South Atlantic (Illig and Bachèlery 2019; Bachèlery et al. 2020).

3.5 Evolving Coastal Topography: Inference on Tides and Waves

While macro-scale global assessments emphasize climate-driven sea level rise as a dominant driver of long-term coastal flood risk (Hinkel et al. 2021), localized coastal bathymetry evolution represents a major compound factor that can significantly amplify or modulate flood severity (Wang et al. 2018). In highly dynamic nearshore systems, short-term local projections of storm flooding are highly sensitive to these morphological adjustments, which can alter tidal dynamics and wave energy dissipation (Rasquin et al. 2020; Wang et al. 2018). Consequently, omitting bathymetric variations can lead to a substantial under- or overestimation of flooding hazards (Gou et al. 2023).

However, uncertainties in topo-bathymetric data are often poorly quantified, outdated, or inaccurate, limiting the reliability of flood projections (Almar et al. 2021). The lack of comprehensive information on coastal processes represents a major source of uncertainty in future coastal flooding assessments (Le Cozannet et al. 2015). Recent advances in satellite-derived topo-bathymetry offer new opportunities to improve boundary conditions in flooding models, especially in the nearshore zone where morphology evolves dynamically. It is important to integrate up-to-date topo-bathymetry estimates into flooding models and compare their performance against coarser or static datasets. Topo-bathymetric uncertainties have a strong control in flooding prediction skills. The level of acceptable accuracy needed will help to define future satellite mission priorities and techniques for accurately monitoring coastal morphologies in flood risk assessments (Vousdoukas et al. 2018).

Accurate coastal topo-bathymetry is fundamental for understanding coastal processes, managing infrastructure, and assessing flooding risks (Benveniste et al. 2019; Cesbron et al. 2021). However, traditional in situ surveys, while precise, are expensive, time-consuming, and often unavailable in remote regions, resulting in sparse coverage beyond localized areas. Satellite-based methods are increasingly addressing this gap, with recent missions offering improved spatial resolution, revisit frequency, and spectral capabilities (Bergsma et al. 2020). Among these, color radiometry (Lyzenga et al. 1978, Caballero ans Stampf, 2020), and other techniques (Almar et al. 2021) leverages wave kinematics observed in Sentinel-2 imagery to estimate depths in the crucial 0–50 m range where wave transformation occurs, now meeting International Hydrographic Organization standards (Almar et al. 2023), with a global coverage (Almar et al. 2025). Complementary approaches such as intertidal beach assessments (Vos et al. 2020) and waterline extraction at varying tidal stages (Bergsma et al. 2024) allow for a more comprehensive representation of coastal morphology, overcoming limitations of static bathymetry methods. Investigating how nearshore morphological variability affects wave run-up and flooding risk is a key objective, as coastal dynamics have been shown to significantly influence flooding projections (Melet et al. 2020a). High-resolution stereo-photogrammetry from Pleiades satellite imagery will further refine topographic data at selected hotspots (Almeida et al. 2019; Taveneau et al. 2021), contributing to more accurate flooding assessments and highlighting the need for improved satellite-derived topo-bathymetry products.

4 Forcing Factors on Coastal Sea Level

This section discusses large-scale climate-related processes that also affect coastal sea level, focusing on interannual-to-decadal time scales.

4.1 Mass and Steric Changes, and Effects of GIA and GRDs

On interannual-to-multidecadal timescales, sea level changes at the coast result from the superposition of different components: the global mean sea level rise, remote regional changes and local variations due to small-scale coastal processes (Cazenave and Moreira 2022).

The two main causes of present-day global mean sea level rise are ocean warming via thermal expansion of seawater and melting of continental ice (glaciers, Greenland and Antarctica), in response to anthropogenic greenhouse gas emissions. Exchange of water between land and ocean also plays a role, although much smaller in terms of trend than thermal expansion and land ice melt. Different observing systems allow us to quantify these contributions (e.g., WCRP, 2018). The international Argo network of about 4000 automatic floats (e.g., Riser et al. 2016) provides ocean temperature and salinity measurements down to 2000 m depth, with near global coverage. In addition, the GRACE space gravimetry mission launched in 2002 and its successor GRACE follow On/FO launched in 2018, measure mass changes in the Earth system (Tapley et al. 2019), including the loss of ice mass in Greenland and Antarctica. Other space techniques such as radar interferometry and radar and laser altimetry are also used to estimate ice mass losses from the polar ice sheets (e.g., WCRP 2018). Recent studies compared the altimetry-based global mean sea level with the sum of contributions and showed closure of the global budget within data uncertainties from 1993–2016 (e.g., Nerem et al. 2018; Hamlington et al. 2020; Horwath et al. 2022). Over this time span, thermal expansion and ocean mass change (mostly due to land ice melt) contribute for ~ 40–60% respectively. For the recent years, instrumental problems affecting the Jason-3 and GRACE/GRACE FO satellites, as well as some missing contributions cause imperfect closure of the global mean sea level budget (e.g., Chen et al. 2020; Barnoud et al. 2021, 2023; Mu et al. 2024). However, correcting for the instrumental drift issues and accounting for the deep ocean warming contribution has now allowed closing the sea level budget since 2017 (Cazenave et al. 2026).

At regional scale, in addition to the global mean ocean thermal expansion and mass increase, spatial trend patterns result from additional components. These include: (1) vertically integrated regional ocean temperature and salinity changes, (2) water mass redistribution by the ocean circulation, (3) GRDs (Gravity, Earth Rotation, and solid Earth Deformations) due to the visco-elastic and elastic response of the crust to past (i.e., GIA) and ongoing land ice melt and associated gravity changes. The largest contribution to regional sea level trends comes from the temperature and salinity variations (called steric effects) mostly driven by ocean circulation. Mass redistribution, GIA and GRDs cause large-scale regional sea level changes, of much smaller amplitude than the steric effects. Closure of the regional sea level budget based on different types of measurements and models is seen in some oceanic regions but not everywhere (Royston et al. 2020; Camargo et al. 2023; Bouih et al. 2025). This potentially results from errors in one or more observing systems, or from missing contributions (e.g., deep ocean warming).

In addition to processes causing the global mean sea level rise and the regional trends, other small-scale phenomena may impact, in the long term, sea level change at the coast.

These include trends in waves, low-frequency atmospheric forcing factors, shelf currents, seawater density change due to freshwater input in river estuaries and deltas (Woodworth et al. 2019; Durand et al. 2019).

In most coastal areas, these phenomena remain poorly known because of lack of direct measurements or imperfect small-scale modeling. Thus assessing coastal sea level budget at the very local scale is not yet possible, although a number of investigations have provided interesting new results on sea level changes over shelf areas in specific oceanic regions, in response to various mechanisms such as wind stress, river runoff, influence of climate modes, etc. (among others, Frederikse et al. 2016, 2018; Han et al. 2019; Wang et al. 2021; Dangendorf et al. 2023; Camargo et al. 2022).

These coastal and shelf processes and how they impact coastal sea level are discussed below.

4.2 Surface Forcings and Climate Modes

Surface wind, sea level pressure and buoyancy flux are key drivers of coastal sea level variability on interannual to multidecadal timescales (Woodworth et al. 2019), producing sea level anomalies that can reach several tenths of a meter (e.g., Sweet et al. 2022; Li et al. 2021). Climate modes, which represent the dominant and recurring patterns of internal climate variability, explain a substantial fraction of the variability in these surface forcing fields and, consequently, in coastal sea level. The influences of climate modes on regional and coastal sea level across different ocean basins, together with the associated

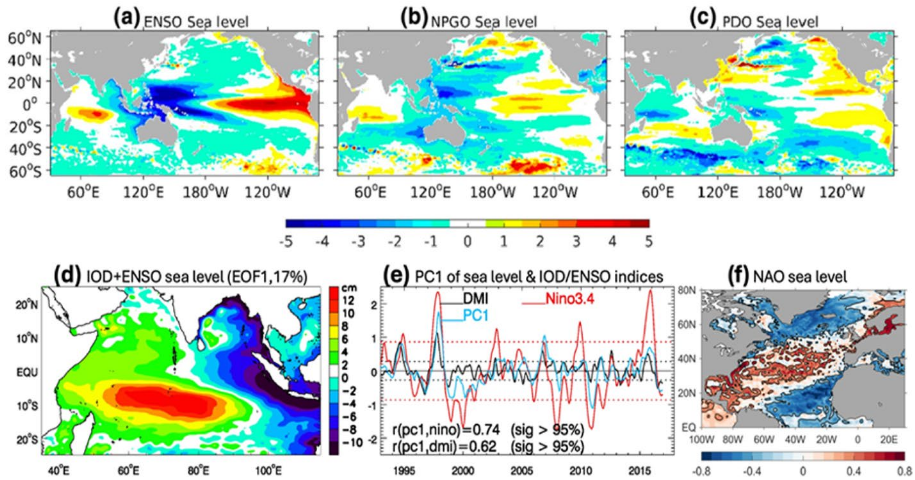

Fig. 11 Regression coefficients of sea level anomaly (SLA; unit: cm) over the Indo-Pacific basin with respect to **a** ENSO, **b** North Pacific Gyre Oscillation (NPGO) and **c** Pacific Decadal Oscillation (PDO) indices based on multiple linear regression analysis of the ECMWF ORAS5 reanalysis data for the 1958–2017 period. **d** The leading Empirical Orthogonal Function (EOF1) pattern of monthly AVISO satellite SLA from 1993–2017 (linear trend and monthly climatology removed); **e** PC1 (blue) of satellite SLA, Dipole Mode Index (DMI; black) and Nino3.4 index (red). Horizontal dashed lines show the ± 1STD of DMI (black) and Nino3.4 (red) index. **f** Correlation map between winter (DJFM mean) NAO index and annual mean AVISO satellite SLA over the Atlantic Ocean for the 1993–2016 period; correlation coefficients of ± 0.3 are shown by the black line contours. Modified from Figs. 2, 7 and 13 of Han et al. (2019)

forcing mechanisms and physical processes, have been comprehensively reviewed by Han et al. (2017, 2019) and Woodworth et al. (2019). Here, we focus on advances reported in the more recent literature.

The best known interannual climate mode is ENSO in the tropical Pacific, with its positive phase being El Niño and negative phase being La Niña. During El Niño, the westerly wind anomalies lower sea level along the coasts of the western tropical Pacific including the South China Sea (Feng et al. 2024a, b), but raise sea level along the North and South American coasts in the eastern Pacific (Fig. 11a). A reversed sea level pattern is induced by La Niña, as shown by the steric sea level anomalies derived from multiple in situ based observational datasets (Kang et al. 2025). ENSO also exerts remote impacts on coastal sea level of the east Indian Ocean through both atmospheric bridge and oceanic connection via the Indonesian Throughflow, increasing (reducing) sea level during La Nina (El Nino) along the coasts of Australia, Indonesia, and the eastern and northern boundaries of the Bay of Bengal (Fig. 11a). Through atmospheric teleconnection, ENSO induces sea level variability along the US Atlantic coast (Arcodia et al. 2024). On decadal timescales, the PDO, together with the North Pacific Gyre Oscillation (NPGO), is associated with significant decadal sea level variability along the west coasts of the North and South Americas in the eastern Pacific, around the islands and coasts of the Southeast Asia and Australia in the western Pacific, and along the coasts of the Indian Ocean (Fig. 11b-c; Deepa and Gnanaseelan 2021).

Over the tropical Indian Ocean, the Indian Ocean Dipole (IOD) induces large-amplitude sea level variability. A positive IOD reduces sea level in coastal Indonesia, Thailand, Myanmar, Bangladesh and India in the eastern basin and increases sea level in the western basin along the coasts of east Africa especially over the Seychelles-Chagoes islands region, a pattern resembling that induced by ENSO (Zhang and Han 2020; Nurlatifah et al. 2021; Barskar et al. 2023; Fig. 11a,d). Indeed, the leading pattern of sea level variability (with trend removed) over the Indian Ocean results from the influences of IOD and ENSO (Fig. 11d,e). The co-occurrences of negative IOD and La Niña promoted compounding height-and-heat extremes in recent decades (Han et al. 2022). On intraseasonal timescales, the strong winds associated with the Madden–Julian Oscillation (MJO) can cause extreme sea level events along the southern coast of Java and Nusa Tenggara during boreal spring (Kamp et al. 2024), and MJO combined with ENSO can have significant impact on U.S. east coast sea level via atmospheric teleconnection (Arcodia et al. 2024).

In the Atlantic Ocean, the NAO contributes to the surface winds and heat fluxes that drive interannual and decadal sea level variability along the west and east coasts of the North Atlantic through both remote and local processes (see reviews by Han et al. 2019 and references therein). A positive NAO decreases (increases) U.S. east coast sea level north (south) of Cape Hatteras (Fig. 11f). The NAO impact on interannual sea level anomalies along the U.S. northeast coast, however, exhibits significant multi-decadal changes, due to NAO-related pattern changes of local longshore wind and sea level pressure (Zhu et al. 2023). Furthermore, the NAO-related surface buoyancy (heat and freshwater) fluxes drive variability in the Atlantic Meridional Overturning Circulation (AMOC), which in turn can affect U.S. east coast sea level, extreme sea level events and floods (e.g., Volkov et al. 2023; Yin, 2021; Zhang et al 2025), although climate model simulations show large spread in the relationship between U.S. east coast sea level and AMOC strength (Little et al. 2019). In the southern part of the Mid-Atlantic Bight, decadal sea level anomalies and the recent accelerated increase in high-tide flooding are strongly influenced by remote impacts of the decadal variability of the IOD, which modulates surface buoyancy fluxes and winds over the North Atlantic via atmospheric teleconnections (Zhu et al. 2024).

Along the North Atlantic's east coast, the NAO had stronger influence in the second half of the twentieth century than the first half, with a positive NAO increasing sea level in the North Sea, northern coasts of Europe and Baltic Sea (e.g., Pham et al. 2024), but reducing sea level in the south as revealed by satellite altimetry data (Fig. 11f). The NAO and the Atlantic Multidecadal Variability (AMV) drive the sea level rise acceleration along the Dutch coast since the 1960s (Keizer et al. 1960), and the AMV is also linked to decadal sea level variability in some coastal areas of the Indian Ocean (Deepa and Gnanaseelan 2021).

In the Southern Hemisphere (SH), surface winds associated with the persistent upward trend of the southern annular mode (SAM) cause rapid sea level rising trends in the SH subtropical oceans, including some coastal regions of the South Africa, Australia and Brazil as shown by satellite altimetry data since 1993 (e.g., Qu et al. 2019; Sun et al. 2022a, b; Schossler et al. 2024) and in situ-based observations from 1958–2014 (Duan et al. 2021).

4.3 Along-Coast Coherence

Studies have investigated the along-coast coherence of interannual sea level variations at the planetary scale (e.g., Oelsmann et al. 2024; Leclercq et al. 2025). Using gridded altimetry data, Oelsmann et al. (2024) demonstrated the coherent influence of ENSO along the eastern Pacific coasts, of NAO and AMO (Atlantic Multidecadal Oscillation) in the

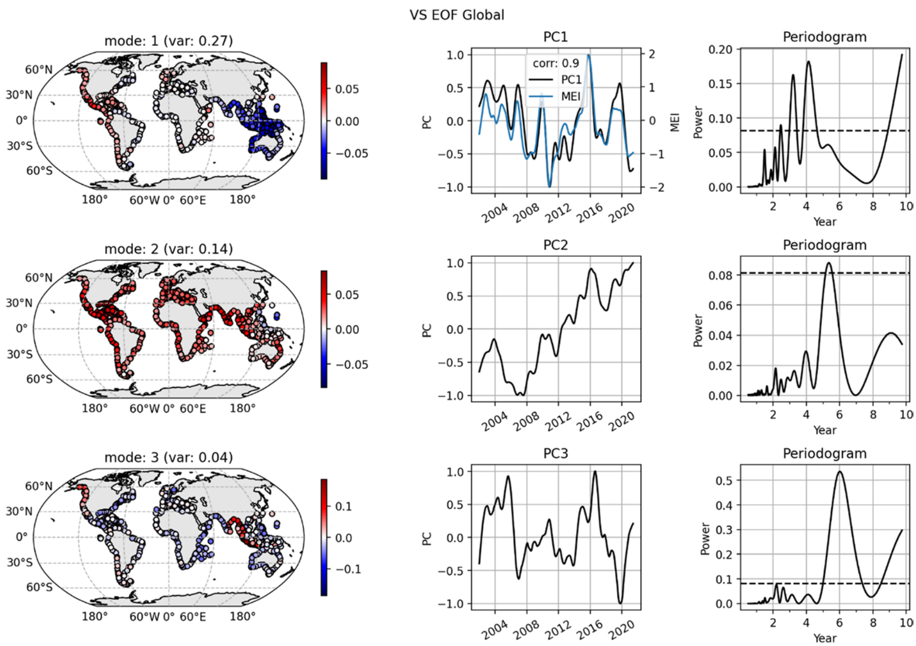

Fig. 12 First three modes of the EOF decomposition of the coastal deseasonalized (but not detrended) sea level time series at 1132 virtual coastal stations. We show for each mode the spatial distribution (left panel), the corresponding PC time series (middle panel) and the PC periodogram (right panel; the dashed line represents the 90% confidence level). MEI (Multivariate ENSO Index) is superimposed on the PC1 time series. The PCs are normalized and the spatial maps are in meters (From Leclercq et al. 2025)

Atlantic and of the IOD in the Indian Ocean, confirming that internal climate modes represent the dominant factors of interannual variability of coastal sea level.

Applying an Empirical Orthogonal Function (EOF) decomposition (Preisendorfer 1988) of coastal sea level time series derived from reprocessed coastal altimetry data over a 20-year long time span (2002–2021), at a set of 1130 + virtual coastal stations (ESA CCI coastal sea level project), Leclercq et al. (2025) also found dominant influence of internal climate modes, in particular ENSO on the interannual coastal sea level variability. But this study also reports novel findings in coastal sea level: (1) a regime shift between 2008 and 2012, with increased sea level rate after that date in many coastal regions, and (2) a 6-year cycle, notably along the northeast and northwest coasts of America (north of 40°) and along the Indian coast of Indonesia. This is illustrated in Fig. 12, showing the first three modes of the EOF decomposition of altimetry-based coastal sea level time series over 2002–2021 at 1130 + virtual coastal stations homogeneously distributed along the world coastlines.

4.4 River Discharge

River discharge, the volume of water flowing in a river cross-section per unit time, represents the primary mechanism through which freshwater is transferred from land to the

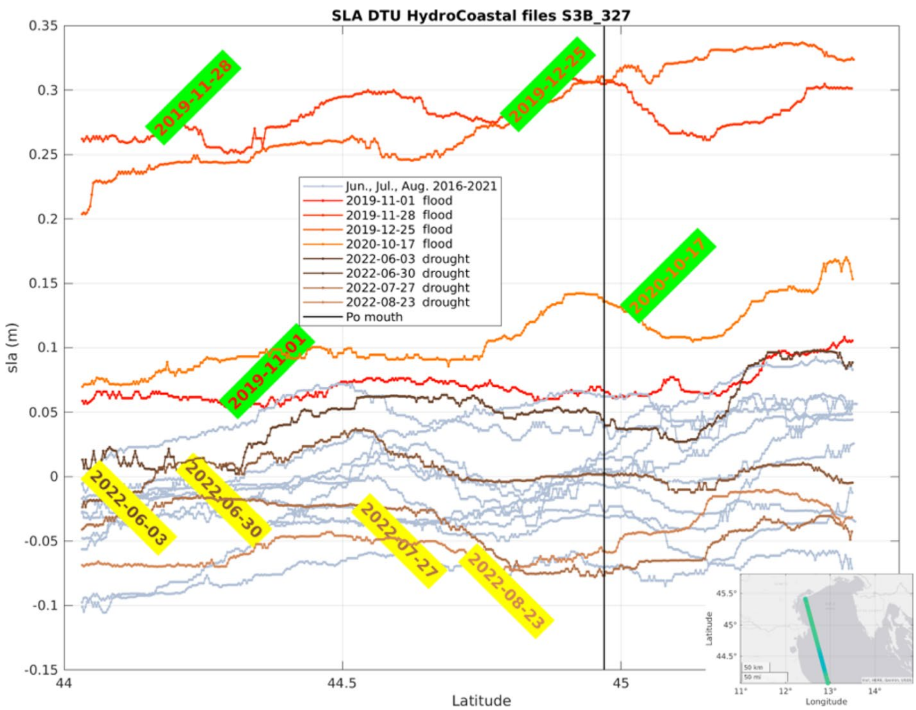

Fig. 13 Sea level anomalies (m) in the coastal area of the Po River delta derived from Sentinel-3 radar altimetry and processed within the ESA–HYDROCOASTAL project. These observations illustrate the variability of coastal sea level in the vicinity of a major river mouth. The inset (bottom right) shows the Sentinel-3 ground track (blue)

oceans. Variations in river discharge are therefore important drivers of coastal sea level variability, linking terrestrial hydrological processes with ocean dynamics (Durand et al. 2019). Recent advances in satellite remote sensing and hydrological modeling now enable river discharge to be monitored with unprecedented spatial and temporal coverage, providing new opportunities to investigate land–ocean freshwater exchanges and their impact on coastal sea level.

Among the most promising recent developments is the SWOT satellite mission, designed to measure river water surface elevation, slope, and width with unprecedented spatial resolution (Fu et al. 2024). SWOT's Ka-band radar interferometric enables discharge estimation for rivers wider than ~ 100 m, while its global wide-swath observations open new frontiers for monitoring freshwater fluxes from land to ocean (Durand et al. 2023; Andreadis et al. 2025). Beyond river discharge estimation, recent studies have demonstrated SWOT's ability to observe the land–ocean continuum, providing accurate measurements of coastal water surface elevation in nearshore and estuarine environments that have traditionally challenged conventional nadir altimeters (Lichtman et al. 2025; Rong et al. 2026). These capabilities enable the investigation of river–ocean interactions, tidal amplitude in estuaries (Hart–Davis et al. 2026), backwater effects, compound flooding, intertidal dynamics (Salameh et al. 2024) and coastal morphodynamic processes, providing an unprecedented observational framework for studying freshwater exchanges between land and ocean.

These fluxes are not only for river hydrology, but also directly influence coastal sea level through two mechanisms (Piecuch et al. 2018): (i) a mass contribution, in which added freshwater increases local sea surface height (Gregory et al. 2019; Piecuch 2023), and (ii) a halosteric effect, in which the introduction of low salinity water alters density gradients, potentially creating floating plumes and baroclinic sea level anomalies (Durand et al. 2019).

The growing body of evidence from studies in the literature highlights the potential of integrated Earth Observation-based approaches to capture these land–ocean interactions (Durand et al 2019; Giffard et al. 2019; Li et al. 2021). Figure 13 highlights coastal sea level anomalies of up to about 50 cm close to the Po River Delta, measured by the ESA Sentinel-3 satellite and associated with variations in river discharge, particularly during high-flow conditions, together with coastal hydrodynamic processes from the ESA-funded HYDROCOASTAL project, https://sentinels.copernicus.eu/web/success-stories/-/copernicus-sentinel-3-altimetry-data-boost-hydrology-studies). Indeed, understanding the role of river discharge in modulating coastal sea level variability is becoming increasingly relevant for climate adaptation and coastal risk assessment. With SWOT and future missions, satellite hydrology is entering a new era in which inland and coastal water processes can be observed as a continuum.

5 Sea Level Modeling (from Global to Local)

Models complement observations. Despite existing technology, some areas remain challenging to monitor adequately due to various factors, such as the complexity of specific phenomena or the unique characteristics of the location (e.g., complex topographies and shorelines) or simply because instruments near coasts are limited. Additionally, where measurements cannot reach, numerical models can help us explore unknown aspects, filling the gaps. Models are also extremely useful for process-based studies.

5.1 Global Ocean Reanalyses

As discussed above, we now have at our disposal a 34-year-long gridded altimetry record, but no gridded sea level dataset is available prior to the 1990s, preventing us from performing long-term analyses. For that reason, ocean reanalysis products—ocean model simulations that are constrained by observed data—are often used in sea level studies, because they provide near-global sea level with relatively long-time span (e.g., since 1950s when more in situ data are available) (Han et al. 2019 and references therein). These global reanalyses also allow assessment of processes causing sea level changes. For instance, the 0.25°, monthly sea level data from the European Centre for Medium-Range Weather Forecasts high-resolution Ocean Reanalysis System 5 (ORAS5) available since 1958 (Zuo et al. 2019), were analyzed in conjunction with satellite altimeter data to study US east coast sea level (Zhu et al. 2024). Note that ORAS5 sea level anomalies have significant differences from tide gauge data in the South Atlantic Bight and Gulf of Maine especially before 1993 (Zhu et al. 2024). Hermans et al. (2020) compared the 1/12° Global Ocean eddy-resolving reanalysis (GLORYS12) data available since 1993 (Lellouche et al. 2018) with satellite altimetry data and their model simulations over the northwest European Shelf, showing good agreements among them.

There are many other reanalysis datasets available that have been used for regional sea level studies in the open ocean. For instance, the Simple Ocean Data Assimilation (SODA) data were used to study multidecadal sea level trend patterns over the Indian Ocean (Han et al. 2010), and the Estimating the Circulation and Climate of the Ocean version 4 (ECCOv4) data were used to study sea level variability over the Arctic Ocean and Nordic Seas (Fukumori et al. 2015). Recently, Bouih et al. (2025) carried out a budget analysis of regional sea level trend over the 2004–2022 period using satellite observations together with six reanalysis datasets all with 0.25° resolution (see their Table 1: GLORYS, C-GLORS, ORAS5, FOAM, SODA and CIGAR). Realistic representation of coastal sea level variations by reanalysis datasets, however, has been challenging partly due to their coarse horizontal resolutions and errors in data assimilation. By comparing six reanalysis data with tide gauge observations, Feng et al (2024a, b) showed that the skill of reanalysis data improves significantly with resolution. In particular GLORYS12 and HYbrid Coordinate Ocean Model (HYCOM) ocean reanalyses, both with eddy-resolving 1/12° resolution and assimilated satellite altimetry data, show more skill than three other ocean reanalyses (ACCESS-S2, ORAS5, and ORAP6) with 0.25° resolution. Lowest skill is observed in the National Centres for Environmental Prediction (NCEP) Climate Forecast System Reanalysis (CFSR) which has 0.5° resolution without altimetry assimilation. These studies suggest that the recently developed high-resolution reanalysis datasets are more skillful in representing coastal sea level variations, which are useful for better understanding the physical processes associated with coastal sea level and flood risks.

For studying extreme sea levels, tides, and storm surges, a global reanalysis dataset has been produced for the period from 1979–2017 using the third generation barotropic Global Tide and Surge Model (GTSM, Muis et al. 2016), with a coastal resolution of 2.5 km (1.25 km in Europe); the data are shown to have good agreement with the observed sea levels from the tide gauge stations in the Global Extreme Sea Level Analysis (GESLA) dataset (Muis et al. 2016). This dataset has been updated for the period from 1950–2024, with horizontal resolution of 0.1° near the coast, and 0.25°, 0.5°, and 1° within 100 km, 500 km, and > 500 km off the coastline, respectively.

Recently, a 43-year (1979–2021) Coastal Ocean Reanalysis (CORA) dataset of hourly coastal water levels for the Gulf of Mexico and U.S. East Coast region has been produced by NOAA (National Oceanic and Atmospheric Administration); it has unstructured grids with varying spatial resolution that averages 400 m near the coast and is much coarser in the open ocean (Rose et al. 2024). It has been shown that the CORA reanalysis data generally perform better than GLORYS12 in capturing the variability on monthly, seasonal, and interannual timescales as well as the long-term trend, and they are used to study extreme water levels and coastal inundations around Miami, Florida to demonstrate an application of CORA for studying flood risks (Rose et al. 2024). The high-resolution reanalysis datasets, combined with satellite and tide gauge observations and model simulations, will improve our understanding of the drivers and processes of regional, coastal sea level variations at a range of timescales. Besides, assimilation of SWOT sea level observations in global ocean reanalyses (e.g., GLORYS12) will allow eddy-resolving modeling. In addition, developing regionally focused coastal reanalysis datasets with spatial resolutions of tens to hundreds of meters (e.g., CORA) would be extremely useful.

5.2 High-Resolution Hydrodynamical Coastal Models

If we exclude models dedicated to surface gravity wave modeling, two kinds of ocean hydrodynamic models can be considered: those representing the barotropic dynamics (where surfaces of constant pressure and surfaces of constant density coincide) and those simulating both barotropic and baroclinic dynamics. The latter are intrinsically three-dimensional.

5.2.1 Barotropic Models

Barotropic models are mostly run to simulate barotropic tides and/or surges. The effect of stratification is neglected or parametrized. Barotropic tidal and/or surge models are used to provide very accurate predictions of sea level, in particular to provide operational corrections for satellite altimetric data. The latter, referred to as the ‘Dynamic Atmospheric Correction/DAC’, accounts for the departure from a pure inverted barometer response to meteorological forcing, mainly over continental shelves and enclosed or semi-enclosed regions (Carrère and Lyard, 2003). The DAC correction is based on the state-of-the-art of modeling and leads to an improvement of 4–5 cm on average and standard meteorological conditions in coastal zones in comparison with the static inverse barometer correction (L. Carrère, pers. comm., 2025). However, the recent SWOT mission provides data with an unprecedented accuracy at small scales which challenges these modeling efforts. For instance, Dibarboure et al. (2025) suggest that SWOT captures the impact of atmospheric orographic waves on sea surface height near the coast and islands at a spatial scale that is not resolved (yet) by the DAC correction. Barotropic surge models are also used in coastal regions to predict coastal flooding in extreme events; in this case, coupling tides and surge models are needed to represent the nonlinear interactions between the processes that may account for a significant part of the sea level increase.(e.g., Idier et al. 2019; Khan et al. 2021)

Overall, one of the most limiting factors for these tides/surges models is the lack of precise information on ocean topography (including intertidal and embankment topography).

Other sources of uncertainty come from the representation of friction, for instance due to wind and waves (Pineau–Guillou et al. 2020) or to the sea ice extent (Cancet et al. 2025).

5.2.2 Baroclinic Models

Baroclinic processes affect vertical stratification, hence tides but also non-tidal processes as dynamic and steric sea levels. Melet et al. (2020a) presented an overview of 3D baroclinic hydrodynamical ocean general circulation models (OGCMs) based on primitive equations used for simulating ocean sea level variations at different time scales at the global scale. The increase of computational capacities and of satellite observations availability and coverage allowed the use of those global models, in combination with data assimilation, to build operational forecasting systems and produce long-term climate projections of regional to global sea level, notably in the CMIP (*Climate Model Intercomparison Project*) framework. Through a 3D nudging to temperature and salinity fields provided by a global 3D baroclinic operational system, Wang and Bernier (2025) also added baroclinicity effects to a global barotropic forecast system. Melet et al. (2020a, 2020b) however underlined that simulating and forecasting sea level at the coast remains challenging, notably due to the wealth and short scales of processes driving coastal sea level and dynamics. This calls for the use of systems specifically designed for those coastal specificities.

Over the last three decades, numerical developments have been made to address this need. 3D regional to coastal models (NEMO, SYMPHONIE, ROMS, HYCOM, CROCO, MITgcm, FVCOM, etc., see Klingbeil et al. 2018 for a review) developed by wide communities of scientists, are now used to study the regional to even estuarine circulation and sea level variability at different and temporal scales, from extreme events to climate change. Those models represent the fine-scale baroclinic physical processes that contribute to the coastal circulation and sea level (meso-to-submesoscale structures, upwellings, coastal and shelf currents, internal tides, waves, river discharges, air-sea interactions…) with different degrees of accuracy depending on their configurations and on the various developments that have been carried out specifically for this purpose. We present here some of the key issues and developments associated with the accurate modeling of coastal dynamics.

Topography plays a major role in the variability of coastal sea level, including the propagation of tides, in particular in shallow areas (estuaries, deltas, gulfs). Piton et al. (2020) for example showed that using an improved bathymetry dataset constructed from local information and GEBCO (Monahan 2008) reduced the simulated tidal amplitude error by up to 60% compared to the use of global datasets. Although satellite data can help to provide the necessary information (see Sect. 3.4), taking into account the past and future changes of bathymetry and coastline due to natural and human factors is also a challenge, both in terms of access to the relevant information and numerical development.

Topography and coastline representation is also a constraint for the design of the numerical grid. On the horizontal dimension, stretched grids as developed by Mathis et al. (2018) are particularly relevant for coastal studies, allowing to considerably improve the detailed representation of topography and resulting coastal dynamics (see e.g. Piton et al. 2020). On the vertical, the use of terrain-following sigma coordinates was developed to better represent topography gradients, but can result in spurious numerical mixing in the presence of steep slopes. Several authors (e.g. Dukhovskoy et al. 2009; Siddorn and Furner 2013; Estournel et al. 2021), thus developed vanishing quasi sigma (VQS) coordinates which still follow the ocean bottom but show noticeably gentler slopes than classical sigma coordinates, allowing to better reproduce the vertical stratification and sea surface characteristics. Another specific constraint of coastal modeling is related to the representation of intertidal zones; moving coastal boundaries indeed influence the absorption of tidal energy and affect horizontal and vertical mixing processes, impacting the amplitude of tidal coastal waves, the bottom stress and surface elevation gradient. Wetting and drying schemes were successfully applied in several coastal areas to address those issues (see e.g. Defne and Ganju 2015; Gräwe et al. 2016).

The advection of tracers in fixed-coordinate models is another major source of spurious numerical mixing (Klingbeil et al. 2019). It is critical in regions of marked topography where powerful internal waves inducing strong vertical mixing are generated, as in the Gibraltar Strait (Chioua et al. 2013) or in the numerous straits of the Southeast Asian seas (Sprintall et al. 2019). Garinet et al. (2024) proposed a new formulation of the advection scheme to address this issue.

As coastal models are usually nested into larger-scale models, a specific challenge arises when downscaling the large-scale information of the variables and of their uncertainty at the open boundaries of the coastal model (e.g., Ghantous et al. 2020–Alvarez Fanjul et al. 2022). The issue of open-boundary conditions is crucial for coastal sea level modeling, not only because they influence the dynamics inside the coastal domain, but also because they directly determine the slow variations of the mean sea level in the domain.

As discussed above, waves also affect the coastal circulation and sea level through the generation of residual flows and turbulence (Uchiyama et al. 2009, 2017; Bertin et al. 2012). The representation of wave–current interactions has been the focus of recent developments (Bennis et al. 2011), and some 3D models account for the effect of waves at different levels of sophistication using wave models (as WW3, Ardhuin et al. 2010 or SWAN, Booij et al. 1999, see below) in forced modes (Uchiyama et al. 2009; Michaud et al. 2012), sometimes including specific parameterizations of the retroaction of the current to Stokes drift (Xu and Bowen 1994; Weiss et al. 2024, 2025); or in fully coupled modes (Uchiyama et al. 2017). More recently, non-hydrostatic baroclinic models (Marshall et al. 1997; Kanarska et al. 2007; Auclair et al. 2011) were also developed to represent phase-resolved waves for coastal sea level management purposes (Marsaleix et al. 2019).

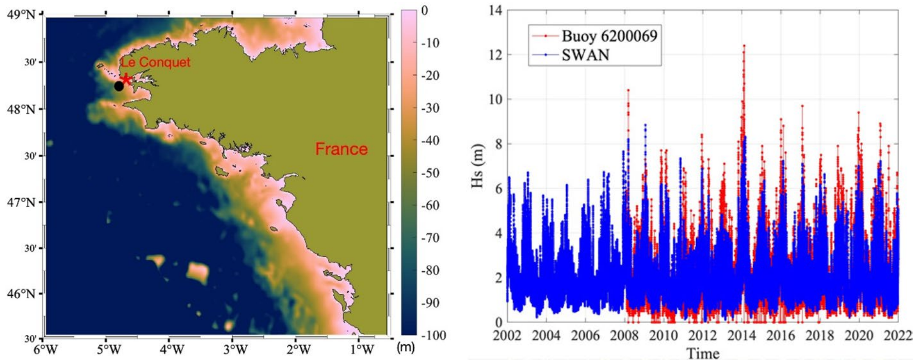

Fig. 14 Simulation region (red star shows the tide gauge site at Le Conquet; black circle shows the nearest wave buoy #6,200,069). SWAN Spectral Wave modeled 1-hourly time series for the Significant Wave height (Hs) in m

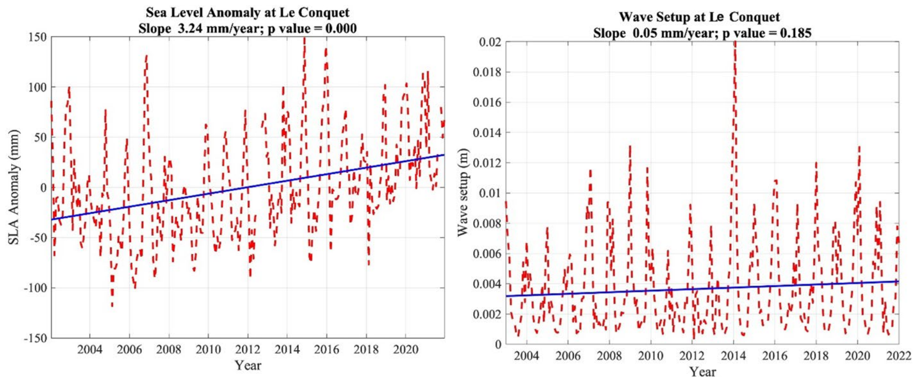

Fig. 15 Sea level anomaly (SLA) time series (red dashed curve) and trend (blue line) using tide gauge data (left); wave setup time series (red dashed curve) and trend (blue line) (right) estimated from the high-resolution SWAN simulations. Location: Le Conquet–France

5.3 Spectral Wave Models

Third-generation spectral wave models are the primary tools for simulating ocean waves and have reached a high level of maturity after several decades of development (WAMDI Group 1988; Komen et al. 1994). Widely used examples include WAM, WAVEWATCH III (WW3), and SWAN, which solve the wave action balance equation to represent wave generation, propagation, nonlinear interactions, and dissipation across global, regional, and coastal domains (Booij et al. 1999; The WAVEWATCH III Development Group, 2016; SWAN Group 2024). These models have become indispensable for operational forecasting, climate studies, wave climate assessments (Dodet et al. 2019), and coastal hazard applications.

Despite their success, important challenges remain. Wave breaking is a highly nonlinear process that remains difficult to parameterize accurately, particularly in shallow-water and surf-zone environments (Cavaleri et al. 2007; McAllister et al. 2024). Similarly, although nonlinear wave–wave interactions are well understood theoretically, their exact numerical solution remains computationally demanding and requires approximations in operational applications.

Recent advances in atmospheric forcing, coastal bathymetry, and data assimilation have substantially improved wave predictions. The assimilation of satellite altimetry, directional wave spectra, and buoy observations has reduced uncertainties in significant wave height and other wave parameters, resulting in more accurate wave analyses and forecasts.

Spectral wave models also provide an essential framework for quantifying wave-driven contributions to coastal sea-level variability. Estimating wave setup, set-down, and run-up enables the assessment of wave contributions to total water levels, coastal flooding, and extreme sea-level events. Recent studies have shown that wave-induced contributions can be comparable to other components of coastal sea-level variability at interannual to decadal timescales (Melet et al. 2018, 2020a,b). At regional and local scales, process-based models such as SWASH and CROCO are increasingly used to resolve surf-zone hydrodynamics and wave run-up processes that spectral wave models cannot represent explicitly (Zijlema et al. 2011; Diaz et al. 2026).

Figures 14 and 15 illustrate a representative application for Le Conquet, on the French Atlantic coast. Figure 14 compares significant wave heights simulated with the SWAN model against buoy observations over the period 2002–2022, demonstrating the ability of modern spectral wave models to reproduce long-term wave variability. The validated wave fields are subsequently used to estimate wave setup and investigate its relationship with sea-level variability derived from the nearby tide gauge. Figure 15 compares the temporal evolution of wave setup and sea-level anomalies.illustrating how spectral wave models, combined with wave-buoy and tide-gauge observations, can be used to assess the contribution of wave-climate variability to long-term coastal sea-level changes.

Future developments will focus on improving the representation of nearshore processes, including wave breaking, shoaling, refraction, wave–current interactions, and compound flooding mechanisms. The integration of high-resolution coastal modeling, expanded satellite observations, and advanced data assimilation techniques is expected to further reduce uncertainties in projections of coastal sea-level extremes and associated hazards.

High-resolution spectral wave models should be further developed and integrated into coastal sea-level studies to better represent wave-induced processes, including wave transformation, setup, runup, and wave–current interactions. When coupled with high-resolution hydrodynamic models and supported by expanding in situ and satellite observations, they will improve our understanding of how waves contribute to coastal sea-level variability and extremes, helping reduce uncertainties in coastal process attribution.

6 Conclusion

Measuring global mean sea level rise and associated regional trends, and understanding underlying causes have considerably improved in recent years, essentially because new in situ and space-based observations have become available. However, this is not the case close to the coasts although coastal sea level rise is a major threat for the world’s low-lying coastal regions. In addition to climate-related sea level rise, coastal zones are also more and more impacted by short-term extreme events, especially when combined with high tides, and in many instances by ground subsidence that amplifies the negative effects of climate change. Adverse effects include temporary and permanent inundation, increased flooding during storm surges, shoreline erosion and retreat, salinisation of wetlands and aquifers, and loss of coastal ecosystems, etc. Coastal zones are densely populated and economically active areas of the world. They concentrate important infrastructures such as harbors and industries. Today, about 600 million people live near the sea, at an altitude less than 10 m above sea level and mostly concentrated in several of the world’s largest megacities. It is now well established that at a local scale, the coastal response to sea level change and extreme events depends on several nonlinearly related factors such as coastal morphology, nearshore bathymetry, sediment supply from rivers, changing waves and currents.

As previously written in Woodworth et al (2019): “The continuity of both in situ and space-based instrumentation is essential for a proper monitoring and understanding changes in sea level”. Indeed, the several techniques used in combination will thereby enable us to understand as well as possible the evolution of coastal zones (Cazenave et al., 2017). It is also essential in order to overcome spatial coverage, resolution and measurement issues for each type of instrument. The coastal virtual station dataset derived from altimetry presented in Sect. 2.2 and tide gauge observations give an example of this complementarity. The redundancy of observations also helps to strengthen resilience of the observing systems to crises. But all recent progress shows that this is the continuity of both (in situ and space-based) instrumentation and models that will allow us to go much further. Indeed, monitoring the different forcing factors described above and understanding their effects on current and future variations in sea level requires an innovative approach that integrates different tools for observing a wide range of parameters, from the global to the local scale, as well as models. Once thoroughly validated, models can fill in the spatial and temporal sparseness of the existing data. This will enable us to understand the processes involved and to predict how the coastal sea level will evolve in the future. This is particularly crucial in the highly-populated world's coastal zones, in order to provide useful information to decision makers in charge of developing adaptation and mitigation strategies to face the many environmental risks faced by coastal regions because of climate change, geohazards and human activities.

Today, thanks to advances in instrumentation, we have an ever-increasing number of in situ measurements of the coastal ocean (greater accuracy, wider spatial and temporal coverage, and new variables), and efforts are being made to integrate these observations into national and international programmes as well as into data dissemination portals (e.g., pan-European JERICO Research Infrastructure, IMOS Australian Ocean Data Network, California Ocean Observing Systems Data Portal). It is essential to emphasize these efforts and ensure their long-term sustainability through appropriate funding mechanisms. At the same time, it is worth noting the density of satellite constellations, the growing diversity of space-based remote sensing instruments (e.g., optical and radar) and the enormous advances in the spatial resolution and temporal frequency of data (e.g., the Copernicus Sentinel-2 mission with a 10-m resolution, the swath altimetry SWOT mission which provides observations at an unprecedented resolution). Space-based data are then increasingly well-suited to observing and monitoring changes in the coastal ocean, including sea level. The exploitation of the latest sensors is only just beginning, and it is still too early to know the new insights they will reveal. While the oceanographic community is very familiar with this type of observation, there is probably still a need to promote it among coastal oceanographers, which will likely require tailored products and training. In parallel, the various sources of satellite data will need to be better combined with one another and/or with in situ measurements and models to improve our understanding of coastal sea levels and the management of their impacts.

Acknowledgements We thank Christopher Piecuch and an anonymous reviewer for their critical comments on the original version of the manuscript. These greatly helped us to improve the content of the paper. We are very grateful to the International Space Science Institute (ISSI) in Bern, Switzerland for having supported our International Team project entitled 'Coastal sea level rise: observations and causes' and organized a team meeting in March 2024 which led to stimulating discussions, at the origin of the present review. This study is partly funded by the ESA Climate Change Initiative Sea Level project (https://climate.esa.int/en/projects/sea-level). R. Almar supported by WACA-VAR and project ANR-22-ASTR-0013–01 GLOBCOASTS. F. Birol and F. Niño are supported by CNES via the TOSCA program (CHARM project). W. Han is supported by the NASA OSTST award 80NSSC21K1190, 80NSSC26K0209 and DOE RGMA DE–SC0024263. M. Herrmann is supported by CNES via the TOSCA program (SEASTERS project) and by IRD via LOTUS international joint laboratory. N. Ayoub is supported by CNES via the TOSCA program (SCOEPUS project) and by CNRS. S. Jevrejeva is supported by NC AtlatniS funding (NE/Y005589/1). L. Leclercq is supported by the ESA CCI Sea Level Project (grant number 4000126561/19–I-NB). J. Oelsmann is supported by European Union's Horizon Europe research and innovation programme. Under the Marie Skłodowska–Curie Grant Agreement No 101210999. F. Papa is supported by CNES via the TOSCA program (SAMBA and FOAM projects). A. Tarpanelli is supported by European Space Agency with the Sentinel-3 and Cryosat SAR/Sarin Radar Altimetry for Coastal Zone and Inland Water Level– HYDROCOASTAL project (4000129872/20/I-DT).S. Ponce de León thanks ESA contract Co. 4000144113/24/1-DT-bgh, awarded for the WAPOSAL project (https://eo4society.esa.int/projects/waposal/). She is currently supported by the European Maritime, Fisheries and Aquaculture Fund (EMFAF) and the "Severo Ochoa Center of Excellence" (CEX2024-001494-S, funded by AEI https://doi.org/10.13039/501100011033) and the MITCAT project (CSIC-PIE-202330E10).

Declarations

Conflict of interest The authors declare no conflict of interest.

References

Ablain M, Meyssignac B, Zawadski L, Jugler R, Ribes A, Spada G, Benveniste J, Cazenave A, Picot N (2019) Uncertainty in satellite estimates of global mean sea-level changes, trend and acceleration. Earth Syst Sci Data 11:1189–1202. https://doi.org/10.5194/essd-11-1189-2019

Adhikari S, Ivins ER, Frederikse T, Landerer FW, Caron L (2019) Sea-level fingerprints emergent from GRACE mission data. Earth Syst Sci Data 11:629–646. https://doi.org/10.5194/essd-11-629-2019

Almar R, Ranasinghe R, Bergsma EWJ et al (2021) A global analysis of extreme coastal water levels with implications for potential coastal overtopping. Nat Commun 12:3775. https://doi.org/10.1038/s41467-021-24008-9

Almar R, Stieglitz T, Addo KA, Ba K, Ondoa GA, Bergsma EW, Arino O (2023) Coastal zone changes in West Africa: challenges and opportunities for satellite earth observations. Surv Geophys 44(1):249–275

Almar R, Bergsma EW, Thoumyre G, Giros A, Marchesiello P, Lemai-Chenevier S, Delvit JM (2025) Global 1-km coastal bathymetry from Sentinel-2 wave inversion using the Satellite-to-Shores (S2hores) Toolbox. Sci Data 12(1):1941

Almeida LP, Masselink G, Russell PE, Davidson MA (2015) Observations of gravel beach dynamics during high energy wave conditions using a laser scanner. Geomorphology 228:15–27. https://doi.org/10.1016/j.geomorph.2014.08.019

Almeida LP et al (2019) Deriving high spatial-resolution coastal topography from sub-meter satellite stereo imagery. Remote Sens 11(5):590

Alvarez Fanjul E, Ciliberti SA, BahurelP (2022) Implementing operational ocean monitoring and forecasting systems; IOC-UNESCO, GOOS-275, 2022. https://doi.org/10.48670/ETOOFS

Alves B, Angnuureng DB, Morand P, Almar R (2020) A review on coastal erosion and flooding risks and best management practices in West Africa: what has been done and should be done. J Coast Conserv 24(3):38

Andreadis KM et al (2025) A first look at river discharge estimation from SWOT satellite observations. Geophys Res Lett 52(9):e2024GL114185. https://doi.org/10.1029/2024GL114185

Ao Z et al (2024) A national-scale assessment of land subsidence in China's major cities. Science 384:301–306. https://doi.org/10.1126/science.adl4366

Arcodia MC, Becker E, Kirtman BP (2024) Subseasonal variability of U.S. coastal sea level from MJO and ENSO teleconnection interference. Weather Forecast 39:441–458

Ardhuin F, Rogers E, Babanin AV, Filipot J, Magne R, Roland A, van der Westhuysen A, Queffeulou P, Lefevre J, Aouf L, Collard F (2010) Semiempirical dissipation source functions for Ocean waves. Part I: definition, calibration, and validation. J Phys Oceanogr 40:1917–1941. https://doi.org/10.1175/2010JPO4324.1

Asher TG, Dusek G, Blanton B, Luettich RA Jr (2020) Mean sea levels, tides, and storm surges, including future projections. Front Mar Sci. https://doi.org/10.3389/fmars.2020.00263

Auclair F, Estournel C, Floor JW, Herrmann M, Nguyen C, Marsaleix P (2011) A non-hydrostatic algorithm for free-surface. Ocean Model 36(1–2):49–70. https://doi.org/10.1016/j.ocemod.2010.09.006
Bachèlery ML, Illig S, Rouault M (2020) Interannual coastal trapped waves in the Angola-Benguela upwelling system and Benguela Niño and Niña events. J Mar Syst 203:103262
Barnoud A, Pfeffer J, Guérou A, Frery M-L, Siméon M, Cazenave A, Chen J, Llovel W, Thierry V, Legeais J-F, Ablain M (2021) Contributions of altimetry and Argo to non-closure of the global mean sea level budget since 2016. Geophys Res Lett 48:e2021GL092824. https://doi.org/10.1029/2021GL092824
Barnoud A, Pfeffer J, Cazenave A, Fraudeau R, Rousseau V, Ablain M (2023) Revisiting the global mean ocean mass budget over 2005–2020. Ocean Sci 19:321–334. https://doi.org/10.5194/os-19-321-2023
Barroso A, Wahl T, Li S, Enriquez A, Morim J, Dangendorf S et al (2024) Observed spatiotemporal variability in the annual sea level cycle along the global coast. J Geophys Res Oceans 129(4):e2023JC020300. https://doi.org/10.1029/2023JC020300
Barskar H, Senapati B, Kaundal M et al (2023) Evolution of tripole pattern of sea-level anomalies in the Indian Ocean during concurrent ENSO-IOD episodes. J Indian Soc Remote Sens 51:383–394. https://doi.org/10.1007/s12524-022-01561-4
Becker M, Papa F, Karpytchev M, Delebecque C, Krien Y, Khan JU, Ballu V, Durand F, Le Cozannet G, Islam AKMS, Calmant S, Shum CK (2020) Water level changes, subsidence, and sea level rise inthe Ganges–Brahmaputra–Meghna delta. Proc Natl Acad Sci U S A. https://doi.org/10.1073/pnas.1912921117
Becker M, Seeger K, Paszkowski A, Marcos M, Papa F, Almar R, Bates P, France-Lanord C, Hossain MS, Khan J, Karegar M, Karpytchev M, Long N, Minderhoud PSJ, Neal J, Nicholls RJ, Syvitski J (2024) Coastal flooding in Asian mega deltas: recent advances, persistent challenges, and call for actions amidst local and global changes. Rev Geophys 62:e2024RG000846. https://doi.org/10.1029/2024RG000846
Bennis AC, Ardhuin F, Dumas F (2011) On the coupling of wave and three-dimensional circulation models: choice of theoretical framework, practical implementation and adiabatic tests. Ocean Model 40(3–4):260–272. https://doi.org/10.1016/j.ocemod.2011.09.003
Benveniste J, Cazenave A, Vignudelli S, Fenoglio-Marc L, Shah R, Almar R et al (2019) Requirements for a coastal hazard observing system, OceanObs'19 community white paper. Front Mar Sci 6(348):2019. https://doi.org/10.3389/fmars.2019.00348
Benveniste J, Birol F, Calafat F, Cazenave A, Dieng H, Gouzenes Y, Legeais JF, Léger F, Niño F, Passaro M, Schwatke C, Shaw A (2020) Coastal sea level anomalies and associated trends from Jason satellite altimetry over 2002–2018. Sci Data 7:357. https://doi.org/10.1038/s41597-020-00694-w
Berghuijs WR, Harrigan S, Molnar P, Slater LJ, Kirchner JW (2019) The relative importance of different flood-generating mechanisms across Europe. Water Resour Res 55(6):4582–4593
Bergsma EW, Almar R (2020) Coastal coverage of ESA'Sentinel 2 mission. Adv Space Res 65(11):2636–2644
Bergsma EW, Klotz AN, Artigues S, Graffin M, Prenowitz A, Delvit JM, Almar R (2024) Shoreliner: a sub-pixel coastal waterline extraction pipeline for multi-spectral satellite optical imagery. Remote Sens 16(15):2795
Bertin X, Bruneau N, Breilh J-F, Fortunato AB, Karpytchev M (2012) Importance of wave age and resonance in storm surges, The case Xynthia, Bay of Biscay. Ocean Model 42(16–30):1463–5003. https://doi.org/10.1016/j.ocemod.2011.11.001
Bevacqua E, Maraun D, Vousdoukas MI, Voukouvalas E, Vrac M, Mentaschi L, Widmann M (2019) Higher probability of compound flooding from precipitation and storm surge in Europe under anthropogenic climate change. Sci Adv 5(9):eaaw5531. https://doi.org/10.1126/sciadv.aaw5531
Birol F, Léger F, Passaro M, Cazenave A, Niño F, Calafat FM, Shaw A, Legeais J-F, Gouzenes Y, Schwatke C, Benveniste J (2021) The X-TRACK/ALES multi-mission processing system: new advances in altimetry towards the coast. Adv Space Res 67:2398–2415. https://doi.org/10.1016/j.asr.2021.01.049
Blewitt G, Kreemer C, Hammond WC, Gazeaux J (2016) MIDAS robust trend estimator for accurate GPS station velocities without step detection. J Geophys Res Solid Earth 121(3):2054–2068. https://doi.org/10.1002/2015JB012552
Booij N, Ris RC, Holthuijsen LH (1999) A third-generation wave model for coastal regions, 1, Model description and validation. J Geophys Res 104:7649–7666
Bouih M, Barnoud A, Yang C, Storto A, Blazquez A, Llovel W, Fraudeau R, Cazenave A (2025) Regional sea level budget over 2004–2022. Ocean Sci 21:1425–1440. https://doi.org/10.5194/os-21-1425-2025
Brempong EK et al (2023) Future flooding of the Volta Delta caused by sea level rise and land subsidence. J Coast Conserv 27(3):142

Bult SV, Le Bars D, Haigh ID, Gerkema T (2024) The effect of the 18.6-year lunar nodal cycle on steric sea level changes. Geophys Res Lett 51:e2023GL106563. https://doi.org/10.1029/2023GL106563
Caballero I, Stumpf RP (2020) Towards routine mapping of shallow bathymetry in environments with variable turbidity: contribution of Sentinel-2A/B satellites mission. Remote Sens 12(3):451
Camargo CML, Riva REM, Hermans THJ, Slangen ABA (2022) Trends and uncertainties of mass-driven sea-level change in the satellite altimetry era. Earth Syst Dyn 13:1351–1375. https://doi.org/10.5194/esd-13-1351-2022
Camargo CML, Riva REM, Hermans THJ, Schütt EM, Marcos M, Hernandez-Carrasco I, Slangen ABA (2023) Regionalizing the sea-level budget with machine learning techniques. Ocean Sci 19:17–41. https://doi.org/10.5194/os-19-17-2023
Cancet M, Lyard FH, Fouchet E (2025) Impact of sea ice friction on ocean tides in the Arctic Ocean, modelling insights at various time and space scales. Ocean Model. https://doi.org/10.1016/j.ocemod.2025.102590
Caron L, Ivins ER, Larour E, Adhikari S, Nilsson J, Blewitt G (2018) GIA model statistics for GRACE hydrology, cryosphere, and ocean science. Geophys Res Lett 45:2203–2212. https://doi.org/10.1002/2017GL07664
Carrere L, Lyard F (2003) Modeling the barotropic response of the global ocean to atmospheric wind and pressure forcing-comparisons with observations. Geophys Res Lett. https://doi.org/10.1029/2002GL016473
Cavaleri L et al (2007) Wave modelling–the state of the art. Prog Oceanogr 75:603–674
Cazenave A, Moreira L (2022) Contemporary sea-level changes from global to local scales: a review. Proc R Soc A Math Phys Eng Sci 478:20220049. https://doi.org/10.1098/rspa.2022.0049
Cazenave A, Le Cozannet G, Benveniste J, Woodworth P, Champollion N (2017) Monitoring the change of coastal zones from space. Eos. https://doi.org/10.1029/2017EO085581
Cazenave A, Gouzenes Y, Birol F, Leger F, Passaro M, Calafat FM, Shaw A, Nino F, Legeais JF, Oelsmann J, Restano M, Benveniste J (2022) Sea level along the world's coastlines can be measured by a network of virtual altimetry stations. Commun Earth Environ 3:117. https://doi.org/10.1038/s43247-022-00448-z
Cazenave A, Yang C, Bouih M, Storto A, Chen J, Llovel W, von Schuckmann K, Leclercq L (2026) Evidence of increased deep ocean warming from a sea level budget approach. Earths Future 14:e2025EF007403. https://doi.org/10.1029/2025EF007403
Cesbron G, Melet A, Almar R, Lifermann A, Tullot D, Crosnier L (2021) Pan-European satellite-derived coastal bathymetry review, user needs and future services. Front Mar Sci 8:740830
Chen JL, Wilson CR, Chambers DP et al (1998) Seasonal global water mass balance and mean sea level variations. Geophys Res Lett 25:3555–3558
Chen JL, Tapley BD, Wilson C, Cazenave A, Seo K-W, Kim JS (2020) Global ocean mass change from GRACE 1 and GRACE Follow-On, and altimeter and Argo measurements. Geophys Res Lett. https://doi.org/10.1029/2020GL090656
Chioua J, Bruno M, Vazquez A, Reyes M, Gomiz JJ, Mananes R, Alvarez O, Gonzalez C, Lopez L, Gomez-Enri J (2013) Internal waves in the Strait of Gibraltar and their role in the vertical mixing processes within the Bay of Algeciras. Estuar Coast Shelf Sci 126:70–86. https://doi.org/10.1016/j.ecss.2013.04.010
Church J et al (2013) Sea level change. In: Stocker T et al (eds) Climate Change 2013: The Physical Science Basis. Contribution of Working Group I to the Fifth Assessment Report of the Intergovernmental Panel on Climate Change (Cambridge University Press, Cambridge, United Kingdom and New York, NY, USA
Collins M et al. (2019) Extremes, Abrupt Changes and Managing Risks. In: IPCC Special Report on the Ocean and Cryosphere in a Changing Climate [Pörtner H-O, Roberts DC, Masson-Delmotte V, Zhai P, Tignor M, Poloczanska E, Mintenbeck K, Alegría A, Nicolai M, Okem A, Petzold J, Rama B, and Weyer NM (eds.)]. In Press, pp 589–656, www.ipcc.ch/srocc/chapter/chapter-6
Dangendorf S, Arns A, Pinto JG, Ludwig P, Jensen J (2016) The exceptional influence of storm 'Xaver' on design water levels in the German Bight. Environ Res Lett 11:054001
Dangendorf S, Marcos M, Wöppelmann G, Conrad CP, Frederiksee T, Riva R (2017) Reassessment of 20th century global mean sea level rise. PNAS 114(23):5946–5951. https://doi.org/10.1073/pnas.16160071
Dangendorf S, Hay C, Calafat FM et al (2019) Persistent acceleration in global sea-level rise since the 1960s. Nat Clim Chang 9:705–710. https://doi.org/10.1038/s41558-019-0531-8
Dangendorf S, Hendricks N, Sun Q, Klinck J, Ezer T, Frederikse T, Calafat FM, Wahl T, Törnqvist TE (2023) Acceleration of U.S. Southeast and Gulf coast sea-level rise amplified by internal climate variability. Nat Commun 14:1935. https://doi.org/10.1038/s41467-023-37649-9

Dangendorf S, Oelsmann J, Mitrovica JX et al (2026) Variable contributions of vertical land motion to sea-level change inferred at tide gauges. Nat Geosci. https://doi.org/10.1038/s41561-026-02005-1
de Lavergne C, Vic C, Madec G, Roquet F, Waterhouse AF, Whalen CB, Cuypers Y, Bouruet-Aubertot P, Ferron B, Hibiya T (2020) A parameterization of local and remote tidal mixing. J Adv Modelling Earth Syst 12:5. https://doi.org/10.1029/2020MS002065
Dean RG, Dalrymple RA (1984) Water wave mechanics for engineers and scientists. Prentice Hall Inc.
Decker M, Brunke MA, Wang Z, Sakaguchi K, Zeng X, Bosilovich MG (2011) Evaluation of the reanalysis products from GSFC, NCEP, and ECMWF using flux tower observations. J Clim 25:1916–1944. https://doi.org/10.1175/JCLI-D-11-00004.1
Deepa JS, Gnanaseelan C (2021) The decadal sea level variability observed in the Indian Ocean tide gauge records and its association with global climate modes, *Global and Planetary Change*, 198. ISSN 103427:0921–8181. https://doi.org/10.1016/j.gloplacha.2021.103427
Defne Z, Ganju NK (2015) Quantifying the residence time and flushing characteristics of a shallow, back-barrier estuary: application of hydrodynamic and particle tracking models. Estuaries Coasts 38:1719–1734
Diaz H, Boucharel J, Marchesiello P, Almar R, Soufflet Y, Benshila R, Almeida LP (2026) Multi-sensor observations and modeling of wave swash on a low-tide terrace beach. Sci Rep. https://doi.org/10.1038/s41598-026-56586-3
Dibarboure G, Anadon C, Briol F, Cadier E, Chevrier R, Delepoulle A, Faugère Y, Laloue A, Morrow R, Picot N, Prandi P, Pujol M-I, Raynal M, Tréboutte A, Ubelmann C (2025) Blending 2D topography images from the Surface Water and Ocean Topography (SWOT) mission into the altimeter constellation with the Level-3 multi-mission Data Unification and Altimeter Combination System (DUACS). Ocean Sci 21:283–323. https://doi.org/10.5194/os-21-283-2025
Dièye A, Marchesiello P, Sow BA, Dieng HB, Thuan DH, Descroix L (2025) Tidal amplification and distortion in Guinea-Bissau, West Africa. Estuar Coast Shelf Sci. https://doi.org/10.1016/j.ecss.2025.109318
Zhu, Yingli, Weiqing Han, Oluwayemi Garuba DL, Suhas, Lai-yung Ruby Leung, Aneesh Subramanian C, Karthik Balaguru, Gengxin Chen, Luke Van Roekel, Jianing Wang (2026) Indian Ocean Dipole and North Atlantic Oscillation as Key Drivers of Accelerated High Tide Flooding along the U.S. East Coast in Recent Decades. Communications Earth & Environment, in revision
Djeumeni Noubissie L, Birol F, Onguene R, Léger F, Niño F, Dzonde Naoussi R (2024) Virtual coastal altimetry tide gauges along the West African coast. Estuar Coast Shelf Sci 296:108600. https://doi.org/10.1016/j.ecss.2023.108600
Dodet G, Castelle B, Masselink G, Pinto SM, Ruiz de Alegría-Arzaburu A, Tomasicchio GR, Harley MD (2019) Beach recovery from extreme storm activity during the 2013–14 winter along the Atlantic coast of Europe. Front Mar Sci 6:154. https://doi.org/10.3389/fmars.2019.00154
De Dominicis M, Wolf J, Jevrejeva S, Zheng P, and Hu Z (2020) Future interactions between sea level rise, tides, and storm surges in the World's Largest Urban Area. Geophys Res Lett, 47(4). https://doi.org/10.1029/2020GL087002
Dronkers J (1986) Tidal asymmetry and estuarine morphology. Neth J Sea Res 20:117–131
Duan J, Li Y, Wang F, Hu A, Han W, Zhang L, Lin P, Rosenbloom N, Meehl GA (2021) Rapid sea-level rise in the Southern-Hemisphere subtropical oceans. J Clim. https://doi.org/10.1175/JCLI-D-21-0248.1
Dukhovskoy DS, Morey SL, Martin PJ, O'Brien JJ, Cooper C (2009) Application of a vanishing, quasi-sigma, vertical coordinate for simulation of high-speed, deep currents over the Sigsbee Escarpment in the Gulf of Mexico. Ocean Model. https://doi.org/10.1016/j.ocemod.2009.02.009
Durand F, Piecuch CG, Becker M, Papa F, Raju SV, Khan JU, Ponte RM (2019) Impact of continental freshwater runoff on coastal sea level. Surv Geophys 40:1437–1466. https://doi.org/10.1007/s10712-019-09536-w
Durand M et al (2023) A framework for estimating global river discharge from the surface water and ocean topography satellite mission. Water Resour Res 59(4):e2021WR031614. https://doi.org/10.1029/2021WR031614
Egbert GD, Ray RD (2000) Significant dissipation of tidal energy in the deep ocean inferred from satellite altimeter data. Nature 405:775–778
Ekman M (1988) The world's longest continuous series of sea level observations, Pure Appl. Geophys 127:73–77
Escudier et al (2018) Satellite radar altimetry: principle, accuracy and precision, in 'Satellite altimetry over oceans and land surfaces, D.L Stammer and A. Cazenave edts., 617 pages, CRC Press, Taylor and Francis Group, Boca Raton, New York, London, ISBN: 13: 978–1–4987–4345–7
Estournel C, Marsaleix P, Ulses C (2021) A new assessment of the circulation of Atlantic and Intermediate Waters in the Eastern Mediterranean. Prog Oceanogr. https://doi.org/10.1016/j.pocean.2021.102673

Farrell WE, Clark JA (1976) On postglacial sea level. Geophys J R Astron Soc 46:647–667. https://doi.org/10.1111/j.1365-246X.1976.tb01252.x
FEMA (2006) Hurricane Katrina Flood Recovery (Mississippi). Federal Emergency Management Agency (FEMA), 47 FEMA
Feng X, Widlansky MJ, Balmaseda MA, Zuo H, Spillman CM, Smith G, Long X, Thompson P, Kumar A, Dusek G, Sweet W (2024a) Improved capabilities of global ocean reanalyses for analysing sea level variability near the Atlantic and Gulf of Mexico Coastal U.S. Front Mar Sci 11:1338626. https://doi.org/10.3389/fmars.2024.1338626
Feng J, Chen Q, Li D, Yang X, Zhao L (2024b) The dominant modes of recent sea level variability from 1993 to 2020 in the China Seas. Glob Planet Change 237:104451. https://doi.org/10.1016/j.gloplacha.2024.104451
Ferrarin C, Bajo M, Benetazzo A, Cavaleri L, Chiggiato J, Davison S, Davolio S, Lionello P, Orlić M, Umgiesser G (2021) Local and large-scale controls of the exceptional Venice floods of November 2019. Prog Oceanogr. https://doi.org/10.1016/j.pocean.2021.102628
Fox-Kemper B et al. (2021) Ocean, Cryosphere and Sea Level Change. In Climate Change 2021: The Physical Science Basis. Contribution of Working Group I to the Sixth Assessment Report of the Intergovernmental Panel on Climate Change [Masson-Delmotte V, Zhai P, Pirani A, Connors SL, Péan C, Berger S, Caud N, Chen Y, Goldfarb L, Gomis MI, Huang M, Leitzell K, Lonnoy E, Matthews JBR, Maycock TK, Waterfield T, Yelekçi O, Yu R, and Zhou B (eds.)]. Cambridge University Press, Cambridge, United Kingdom and New York, NY, USA, pp. 1211–1362, https://doi.org/10.1017/9781009157896.011
Frankcombe LM, McGregor S, England MH (2015) Robustness of the modes of Indo-Pacific sea level variability. Clim Dyn 45(5–6):1281–1298
Frederikse T, Riva R, Kleinherenbrink M, Wada Y, van den Broeke M, Marzeion B (2016) Closing the sea level budget on a regional scale: trends and variability on the Northwestern European continental shelf. Geophys Res Lett 43:10,864-10,872. https://doi.org/10.1002/2016GL070750
Frederikse T, Jevrejeva S, Riva REM, Dangendorf S (2018) A consistent sea-level reconstruction and its budget on basin and global scales over 1958–2014. J Clim 31(3):1267–1280
Frederikse T, Landerer FW, Caron L (2019) The imprints of contemporary mass redistribution on local sea level and vertical land motion observations. Solid Earth Discuss 10:1971–1987. https://doi.org/10.5194/se-10-1971-2019
Frederikse T, Landerer F, Caron L et al (2020) The causes of sea-level rise since 1900. Nature 584:393–397. https://doi.org/10.1038/s41586-020-2591-3
Fu LL (2003) Wind-forced intraseasonal sea level variability of the extratropical oceans. J Phys Oceanogr 33(2):436–449. https://doi.org/10.1175/1520-0485
Fu L-L, Pavelsky T, Cretaux J-F, Morrow R, Farrar JT, Vaze P et al (2024) The Surface Water and Ocean Topography Mission: a breakthrough in radar remote sensing of the ocean and landsurface water. Geophys Res Lett 51:e2023GL107652. https://doi.org/10.1029/2023GL107652
Fukumori I, Wang O, Llovel W, Fenty I, Forget G (2015) A near-uniform fluctuation of ocean bottom pressure and sea level across the deep ocean basins of the Arctic Ocean and the Nordic Seas. Prog Oceanogr 134:152–172
Garinet A, Herrmann M, Marsaleix P, Pénicaud J (2024) Spurious numerical mixing under strong tidal forcing: a case study in the south-east Asian seas using the Symphonie model (v3.1.2). Geosci Model Dev 17:6967–6986. https://doi.org/10.5194/gmd-17-6967-2024
Gelaro R et al (2017) The modern-era retrospective analysis for research and applications, version 2 (MERRA-2). J Clim 30:5419–5454. https://doi.org/10.1175/JCLI-D-16-0758.1
Ghantous M, Ayoub N, De Mey-Frémaux P, Vervatis V, Marsaleix P (2020) Ensemble downscaling of a regional ocean model. Ocean Model. https://doi.org/10.1016/j.ocemod.2019.101511
Giffard P, Llovel W, Jouanno J, Morvan G, Decharme B (2019) Contribution of the Amazon River discharge to regional sea level in the tropical Atlantic Ocean. Water 11(11):2348
Gobron K, de Viron O, Wöppelmann G, Poirier É, Ballu V, Van Camp M (2019) Assessment of tide gauge biases and precision by the combination of multiple collocated time series. J Atmos Ocean Technol 36:1983–1996. https://doi.org/10.1175/JTECH-D-18-0235.1
Gonzalez NM, Waldman R, Sannino G, Giordani H, Somot S (2023) Understanding Tidal mixing at the strait of Gibraltar: a high-resolution model approach. Prog Oceanogr 2023(212):102980. https://doi.org/10.1016/j.pocean.2023.102980
Gou X, Liang H, Cai T, Wang X, Chen Y, Xia X (2023) The impact of coastline and bathymetry changes on the storm tides in Zhejiang coasts. J Mar Sci Eng 11(9):1832

Gravelle M, Wöppelmann G, Gobron K, Altamimi Z, Guichard M, Herring T, Rebischung P (2023) The ULR-repro3 GPS data reanalysis and its estimates of vertical land motion at tide gauges for sea level science. Earth Syst Sci Data 15(1):497–509. https://doi.org/10.5194/essd-15-497-2023
Gräwe U, Flöser G, Gerkema T, Duran-Matute M, Badewien T, Schulz E, Burchard H (2016) A numerical model for the entire Wadden Sea: skill assessment and analysis of hydrodynamics. J Geophys Res 121:5231–5251
Gregory JM et al (2019) Concepts and terminology for sea level: mean, variability and change, both local and global. Surv Geophys 40:1251–1289. https://doi.org/10.1007/s10712-019-09525-z
Guérou A, Meyssignac B, Prandi P, Ablain M, Ribes A, Bignalet-Cazalet F (2023) Current observed global mean sea level rise and acceleration estimated from satellite altimetry and the associated measurement uncertainty. Ocean Sci 19:431–451. https://doi.org/10.5194/os-19-431-2023
Guza RT, Feddersen F (2012a) Effect of wave frequency and directional spread on shoreline runup. Geophys Res Lett 39:L11607. https://doi.org/10.1029/2012GL052124
Guza RT, Feddersen F (2012b) Effect of wave frequency and directional spread on shoreline runup. Geophys Res Lett 39:2012GL051959. https://doi.org/10.1029/2012GL051959
Haigh ID, Pickering MD, Green JAM, Arbic BK, Arns A, Dangendorf S et al (2019) The tides they are a-changin': a comprehensive review of past and future nonastronomical changes in tides, their driving mechanisms and future implications. Rev Geophys 57:e2018RG000636. https://doi.org/10.1029/2018RG000636
Haigh ID, Eliot M, and Pattiaratchi C (2011) Global influences of the 18.61 year nodal cycle and 8.85 year cycle of lunar perigee on high tidal levels. J Geophys Res 116, C06025, https://doi.org/10.1029/2010JC006645
Hamlington BD et al (2020) Understanding of contemporary regional sea-level change and the implications for the future. Rev Geophys 58:e2019RG000672. https://doi.org/10.1029/2019RG000672
Hammond WC, Blewitt G, Kreemer C, Nerem RS (2021) GPS imaging of global vertical land motion for studies of sea level rise. J Geophys Res Solid Earth 126(7):e2021JB022355. https://doi.org/10.1029/2021JB022355
Han W, Meehl G, Rajagopalan B et al (2010) Patterns of Indian Ocean sea-level change in a warming climate. Nat Geosci 3:546–550. https://doi.org/10.1038/ngeo901
Han W, Meehl G, Stammer D, Hu A, Hamlington B, Kenigson J et al (2017) Spatial patterns of sea level variability associated with natural internal climate modes. Surv Geophys 38(1):217–250. https://doi.org/10.1007/s10712-016-9386-y
Han W, Stammer D, Thompson P, Ezer T, Palanisamy H, Zhang X, Domingues CM, Zhang L, Yuan D (2019) Impacts of basin-scale climate modes on coastal sea level: a review. Surv Geophys 40:1493–1541. https://doi.org/10.1007/s10712-019-09562-8
Han W, Zhang L, Meehl GA, Kido S, Tozuka T, Li Y, McPhaden MJ, Hu A, Cazenave A, Rosenbloom N, Strand G, West BJ, Xing W (2022) Sea level extremes and compounding marine heatwaves in coastal Indonesia. Nat Commun 13:6410. https://doi.org/10.1038/s41467-022-34003-3
Hao Z, Singh V, Hao F (2018) Compound extremes in hydroclimatology: a review. Water 10:718. https://doi.org/10.3390/w10060718
Hart-Davis MG, Scherer D, Schwatke C et al (2026) Observing the tidal pulse of rivers from wide-swath satellite altimetry. Nature 652:371–378. https://doi.org/10.1038/s41586-026-10287-z
Hasselmann K (1962) On the non-linear energy transfer in a gravity-wave spectrum. Part 1. General theory. J Fluid Mech 12:481–500
Hauser L, Boni R, Minderhoud PS, Teatini P, Woillez MN, Almar R, Addo KA (2023) A scoping study on coastal vulnerability to relative sea-level rise in the Gulf of Guinea. AFD Res Pap 283:1–42
Hermans THJ, Le Bars D, Katsman CA, Camargo CML, Gerkema T, Calafat FM et al (2020) Drivers of interannual sea level variability on the northwestern European shelf. J Geophys Res Oceans 125:e2020JC016325. https://doi.org/10.1029/2020JC016325
Herrmann M, To Duy T, Estournel C (2023) Intraseasonal variability of the South Vietnam upwelling, South China Sea: influence of atmospheric forcing and ocean intrinsic variability. Ocean Sci 19:453–467. https://doi.org/10.5194/os-19-453-2023
Herrmann M, To Duy T, Marsaleix P (2024) Mechanisms and intraseasonal variability in the South Vietnam Upwelling, South China Sea: the role of circulation, tides, and rivers. Ocean Sci 20:1013–1033. https://doi.org/10.5194/os-20-1013-2024
Hersbach H et al (2019) Global reanalysis: goodbye ERA-Interim, hello ERA5. Meteorol Appl 59:17–24
Hersbach H, Bell B, Berrisford P et al (2020) The ERA5 global reanalysis. Q J R Meteorol Soc 146:1999–2049. https://doi.org/10.1002/qj.3803
Hightower et al (2026) Impact of heterogeneous mantle viscosity on the glacial isostatic adjustment correction for GRACE(-FO): implications for surface mass trends, submitted. J Geophys Res

Hinkel J, Feyen L, Hemer M, Le Cozannet G, Lincke D, Marcos M, Wolff C (2021) Uncertainty and bias in global to regional scale assessments of current and future coastal flood risk. Earths Future 9(7):e2020EF001882

Hoeke et al (2013) New data systems and products at the permanent service for mean sea level. J Coastal Res 29(3):493–504. https://doi.org/10.2112/JCOASTRES-D-12-00175.1

Hoffmann L, Günther G, Li D, Stein O, Wu X, Griessbach S, Heng Y, Konopka P, Müller R, Vogel B, Wright JS (2019) From ERA-Interim to ERA5: the considerable impact of ECMWF's next-generation reanalysis on Lagrangian transport simulations. Atmos Chem Phys 19:3097–3124. https://doi.org/10.5194/acp-19-3097-2019

Holgate SJ, Matthews A, Woodworth PL, Rickards LJ, Tamisiea ME, Bradshaw E, Foden PR, Gordon KM, Jevrejeva S, Pugh J (2013) New Data systems and products at the permanent service for mean sea level. Coastal Res 29:493–504. https://doi.org/10.2112/JCOASTRES-D-12-00175.1

Holman RA (1986a) Extreme value statistics for wave run-up on a natural beach. Coast Eng 9:527–544. https://doi.org/10.1016/0378-3839(86)90002-5

Holman RA (1986b) Extreme value statistics for wave run-up on a natural beach. Coast Eng 9(6):527–544

Horwath M et al (2022) Global sea-level budget and ocean-mass budget, with a focus on advanced data products and uncertainty characterization. Earth Syst Sci Data 14:411–447. https://doi.org/10.5194/essd-14-411-2022

Hughes CW, Thompson K, Minobe S, Fukumori I, Griffies S, Huthnance J, Spence P (2019) Sea level and the role of coastal-trapped waves in mediating the interaction between the coast and open ocean. Surv Geophys. https://doi.org/10.1007/s10712-019-09535-x

Idier D, Paris F, Le Cozannet G, Boulahya F, Dumas F (2017) Sea-level rise impacts on the tides of the European shelf. Cont Shelf Res 137:56–71. https://doi.org/10.1016/j.csr.2017.01.007

Idier D, Bertin X, Thompson P, Pickering MD (2019) Interactions between mean sea level, tide, surge, waves and flooding: mechanisms and contributions to sea level variations at the coast. Surv Geophys 40(6):1603–1630. https://doi.org/10.1007/s10712-019-09549-5

Illig S, Bachèlery ML (2019) Propagation of subseasonal equatorially-forced coastal trapped waves down to the Benguela upwelling system. Sci Rep 9:5306. https://doi.org/10.1038/s41598-019-41847-1

Intergovernmental Oceanographic Commission (IOC) (1985) Manual on Sea Level 799 Measurement and Interpretation (Volume I—Basic Procedures). Intergov. Oceanogr. Comm. 800 Manuals and Guides, 14, UNESCO, Paris, http://www.psmsl.org/train_and_info/training/manuals/ioc_14i.pdf

Intergovernmental Oceanographic Commission (IOC) (2016) Manual on sea level measurement and interpretation. Volume V - Radar gauges. IOC Manuals and Guides 14, UNESCO, 220

IPCC (2019) IPCC Special Report on the Ocean and Cryosphere in a Changing Climate [Pörtner H-O, Roberts DC, Masson-Delmotte V, Zhai P, Tignor M, Poloczanska E, Mintenbeck K, Alegría A, Nicolai M, Okem A, Petzold J, Rama B, Weyer NM (eds.)]. In press

IPCC (2022a) Extremes, abrupt changes and managing risks. In The Ocean and cryosphere in a changing climate: special report manuscript submitted to Geophysical Research Letters 431 of the Intergovernmental Panel on Climate Change (pp 589–656). Cambridge: Cambridge 432 University Press. https://doi.org/10.1017/9781009157964.008

IPCC (2022b) Sea Level rise and implications for low-lying islands, coasts and communities. In The Ocean and 426 Cryosphere in a Changing climate: special report of the Intergovernmental Panel on 427 Climate Change (pp 321–446). chapter, Cambridge: Cambridge University Press. 428 https://doi.org/10.1017/9781009157964.006 429 20

Jevrejeva S, Moore JC, Grinsted A, Woodworth PL (2008) Recent global sea level acceleration started over 200 years ago? Geophys Res Lett 35:L08715. https://doi.org/10.1029/2008GL033611

Kamp W, Han W, Kido S, Zhang L, McCreary JP (2024) Atmospheric intraseasonal oscillations leading to sea level extremes off the Indonesian coasts bordering the Indian Ocean in recent decades. J Clim 37:2867–2880

Kanarska Y, Shchepetkin A, McWilliams JC (2007) Algorithm for non-hydrostatic dynamics in the Regional Oceanic modelling system. Ocean Model 18(3–4):143–174. https://doi.org/10.1016/j.ocemod.2007.04.001

Kang J, Cha H, Moon J-H (2025) Characteristics of global sea level changes during ENSO periods. Ocean Polar Res. https://doi.org/10.4217/OPR.2025002

Kataraihya D, Wdowinski S (2026) Wind impact on sea level variability along the US Atlantic and Gulf coasts: implications to coastal flooding hazard. Nat Hazards 122:294. https://doi.org/10.1007/s11069-026-08041-9

Keizer I, Le Bars D, de Valk C, Jüling A, van de Wal R, Drijfhout S (1960) The acceleration of sea-level rise along the coast of the Netherlands started in the 1960s. Ocean Sci 19:991–1007. https://doi.org/10.5194/os-19-991-2023

Kemp AC, Horton B, Donnelly JP, Mann ME, Vermeer M, Rahmstorf S (2011) Climate related sea level variations over the past two millennia. PNAS. https://doi.org/10.1073/pnas.1015619108
Khan MJU, Durand F, Bertin X, Testut L, Krien Y, Islam AKMS, Pezerat M, Hossain S (2021) Towards an efficient storm surge and inundation forecasting system over the Bengal delta: chasing the Supercyclone Amphan. Nat Hazards Earth Syst Sci 21:2523–2541. https://doi.org/10.5194/nhess-21-2523-2021
Kleinherenbrink M, Riva R, Frederikse T (2018) A comparison of methods to estimate vertical land motion trends from GNSS and altimetry at tide gauge stations. Ocean Sci 14(2):187–204. https://doi.org/10.5194/os-14-187-2018
Klingbeil K, Debreu L, Lemarié F, Burchard H (2018) The numerics of hydrostatic structured-grid coastal ocean models: state of the art and future perspectives. Ocean Model 125:80–105. https://doi.org/10.1016/j.ocemod.2018.01.007
Klingbeil K, Burchard H, Danilov S, Goetz C, and Iske A (2019) Reducing spurious diapycnal mixing in Ocean Models, in: Energy Transfers in Atmosphere and Ocean, edited by Eden C and Iske A, Mathematics of Planet Earth, Springer International Publishing, Cham, 245–286, ISBN 978–3–030–05704–6, https://doi.org/10.1007/978-3-030-05704-6_8
Kobayashi S et al (2015) The JRA-55 reanalysis: general specifications and basic characteristics. J Meteorol Soc Japan 93:5–48. https://doi.org/10.2151/jmsj.2015-001
Kolker AS, Hameed S (2007) Meteorologically driven trends in sea level rise. Geophys Res Lett 34:2007GL031814. https://doi.org/10.1029/2007GL031814
Komen GJ, Cavaleri L, Donelan MA, Hasselmann K, Hasselmann S, Janssen PAEM (1994) Dynamics and modelling of ocean waves. Cambridge University Press, Cambridge, UK
Le Cozannet G et al (2015) Vertical ground motion and historical sea-level records in Dakar (Senegal). Environ Res Lett 10(8):084016
Leclercq L, Dieng H, Cazenave A et al (2025) Spatio-temporal changes in interannual sea level along the world coastlines. Glob Planet Change 253:104972. https://doi.org/10.1016/j.gloplacha.2025.104972
Legeais JF et al (2018) An improved and homogeneous altimeter sea level record from the ESA Climate Change Initiative. Earth Syst Sci Data 10:281–301. https://doi.org/10.5194/essd-10-281-2018
Lellouche J, Greiner E, Le Galloudec O, Garric G, Regnier C, Drevillon M et al (2018) Recent updates to the Copernicus Marine Service global ocean monitoring and forecasting real-time 1/12 high-resolution system. Ocean Sci 14(5):1093–1126. https://doi.org/10.5194/os-14-1093-2018
Lentz SJ (2024) The coastal sea-level response to wind stress in the Middle Atlantic Bight. J Geophys Res Oceans 129:e2024JC021269. https://doi.org/10.1029/2024JC021269
Li Z, Lian T, Ying J, Zhu X, Papa F, Xie H, Long Y (2021) The cause of an extremely low salinity anomaly in the Bay of Bengal in the spring of 2012, J Geophys Res: Oceans, 126, e2021JC017361. https://doi.org/10.1029/2021JC017361
Lichtman ID, Bell PS, Gommenginger C, Banks C, Calafat FM, Brown J, Williams SDP (2025) Evaluating water levels from the surface water and ocean topography (SWOT) mission in a hyper-tidal coastal and estuarine environment. Earth Space Sci 12:e2024EA004104. https://doi.org/10.1029/2024EA004104
Little CM, Hu A, Hughes CW, McCarthy GD, Piecuch CG, Ponte RM, Thomas MD (2019) The relationship between U.S. East Coast sea level and the Atlantic Meridional Overturning Circulation: a review. J Geophys Res Oceans. https://doi.org/10.1029/2019JC015152
Liu WC, Huang WC (2019) Influences of sea level rise on tides and storm surges around the Taiwan coast. Cont Shelf Res 173:56–72. https://doi.org/10.1016/j.csr.2018.12.009
Llovel W, Penduff T, Meyssignac B, Molines J, Terray L, Bessières L, Barnier B (2018) Contributions of Atmospheric forcing and chaotic ocean variability to regional sea level trends over 1993–2015. Geophys Res Lett. https://doi.org/10.1029/2018GL080838.4
Lyard FH, Le Provost C (1997) Energy budget of the tidal hydrodynamic model FES94.1. Geophys Res Lett 24:687–690
Lyard FH, Allain DJ, Cancet M, Carrère L, Picot N (2021) FES2014 global ocean tide atlas: design and performance. Ocean Sci 17:615–649. https://doi.org/10.5194/os-17-615-2021
Lyzenga DR (1978) Passive remote sensing techniques for mapping water depth and bottom features. Appl Opt 17(3):379–383
Manney GL et al (2017) Reanalysis comparisons of upper tropospheric–lower stratospheric jets and multiple tropopauses. Atmos Chem Phys 17:11541–11566. https://doi.org/10.5194/acp-17-11541-2017
Marcos M, Woodworth PL (2017) Spatio-temporal changes in extreme sea levels along the coasts of the North Atlantic and the Gulf of Mexico. J Geophys Res Oceans 122:7031–7048. https://doi.org/10.1002/2017JC013065

Marcos M, Rohmer J, Vousdoukas MI, Mentaschi L, Le Cozannet G, Amores A (2019) Increased extreme coastal water levels due to the combined action of storm surges and wind waves. Geophys Res Lett 46(8):4356–4364. https://doi.org/10.1029/2019GL082599

Marsaleix P, Michaud H, Estournel C (2019) 3D phase-resolved wave modelling with a non-hydrostatic ocean circulation model. Ocean Model 136:28–50. https://doi.org/10.1016/j.ocemod.2019.02.002

Marshall J, Hill C, Perelman L, Adcroft A (1997) Hydrostatic, quasi-hydrostatic, and nonhydrostatic ocean modelling. J Geophys Res 102:5733–5752

Martín Míguez B, Testut L, Wöppelmann G (2012) Performance of modern tide gauges: towards mm-level accuracy. Sci Mar 76(S1):221–228

Masselink G, Russell P (2013) Impacts of climate change on coastal erosion. Mar Geol 352:1–20

IPCC V Masson-Delmotte P Zhai A Pirani SL Connors C Péan S Berger N Caud Y Chen L Goldfarb MI Gomis M Huang K Leitzell E Lonnoy JBR Matthews TK Maycock T Waterfield O Yelekçi R Yu B Zhou Eds 2021 Climate change 2021: the physical science basis. Contribution of working group I to the sixth assessment report of the Intergovernmental Panel on Climate Change Cambridge University Press

Mathis M, Elizalde A, Mikolajewicz U (2018) Which complexity of regional climate system models is essential for downscaling anthropogenic climate change in the Northwest European Shelf? Clim Dyn 50(7–8):2637–2659. https://doi.org/10.1007/s00382-017-3761-3

McAllister ML, Draycott S, Calvert R et al (2024) Three-dimensional wave breaking. Nature 633:601–607. https://doi.org/10.1038/s41586-024-07886-z

Melet A, Meyssignac B, Almar R, Le Cozannet G (2018) Under-estimated wave contribution to coastal sea-level rise. Nat Clim Change 8:234–239. https://doi.org/10.1038/s41558-018-0088-y

Melet A, Almar R, Hemer M, Le Cozannet G, Meyssignac B, Ruggiero P (2020a) Contribution of wave setup to projected coastal sea level changes. J Geophys Res Oceans 125:e2020JC016078. https://doi.org/10.1029/2020JC016078

Melet A, Teatini P, Le Cozannet G, Jamet C, Conversi A, Benveniste J, Almar R (2020b) Earth observations for monitoring marine coastal hazards and their drivers. Surv Geophys 41:1489–1534. https://doi.org/10.1007/s10712-020-09594-5

Melet A, Pérez Gómez B, and Matte P (2024a) Numerical models for monitoring and forecasting sea level: a short description of present status, State Planet Discuss. [preprint], https://doi.org/10.5194/sp-2024-27

Melet A et al (2024b) Sea level rise in Europe: observations and projections, in: sea level rise in Europe: 1st Assessment Report of the Knowledge Hub on Sea Level Rise (SLRE1), edited by: van den Hurk B, Pinardi N, Kiefer T, Larkin K, Manderscheid P, and Richter K, Copernicus Publications, State Planet, 3-slre1, 4, https://doi.org/10.5194/sp3-slre1-4-2024

Michaud H, Marsaleix P, Leredde Y, Estournel C, Bourrin F, Lyard F, Mayet C, Ardhuin F (2012) Three-dimensional modelling of wave-induced current from the surf zone to the inner shelf. Ocean Sci 8:657–681. https://doi.org/10.5194/os-8-657-2012

Milne G, Gehrels W, Hughes C et al (2009) Identifying the causes of sea-level change. Nature Geosci 2(471–478):583. https://doi.org/10.1038/ngeo544

Minderhoud PSJ, Shirzaei M, Teatini P (2025) From InSAR-derivedsubsidence to relative sea-level rise—a call for rigor. Earths Future 13:e2024EF005539. https://doi.org/10.1029/2024EF005539

Minderhoud PSJ, Erkens G, Pham VH, Bui VT, Erban L, Kooi H and E Stouthamer E (2017) Impacts of 25 years of groundwater extraction on subsidence in the Mekong delta, Vietnam, Environ Res Lett 12 064006, https://doi.org/10.1088/1748-9326/aa7146

Minster JF, Cazenave A, Rogel P (1999) Annual cycle in mean sea level from Topex-Poseidon and ERS-1: inference on the global hydrological cycle. Glob Planet Change 20:57–66

Mitrovica JX, Milne GA (2003) On post-glacial sea level: I. General theory. Geophys J Int 154(2):253–267. https://doi.org/10.1046/j.1365-246X.2003.01942.x

Mitrovica J, Tamisiea M, Davis J et al (2001) Recent mass balance of polar ice sheets inferred from patterns of global sea-level 581 change. Nature 409:1026–1029. https://doi.org/10.1038/3505905458224

Monahan D (2008) Mapping the floor of the entire world ocean: the general bathymetric chart of the ocean. J Ocean Tech 3:108

Morrow R, Fu LL, Ardhuin F, Benkiran M, Chapron B, Cosme E, d'Ovidio F, Farrar JT, Gille ST, Lapeyre G, Le Traon PY (2019) Global observations of fine-scale ocean surface topography with the surface water and Ocean topography (SWOT) mission. Front Marine Sci 15(6):232

Mostert W, Popinet S, Deike L (2022) High-resolution direct simulation of deep water breaking waves: transition to turbulence, bubbles and droplets production. J Fluid Mech 942:A27

Mu D, Church JA, King M, Ludwigsen CB, Xu T (2024) Contrasting discrepancy in the sea level budget between the North and South Atlantic Ocean since 2016. Earth Space Sci 11:e2023EA003133. https://doi.org/10.1029/2023EA003133
Muis S, Verlaan M, Winsemius H et al (2016) A global reanalysis of storm surges and extreme sea levels. Nat Commun 7:11969. https://doi.org/10.1038/ncomms11969
Müller M, Cherniawsky JY, Foreman MGG, von Storch J-S (2014) Seasonal variation of the M2 tide. Ocean Dyn 64:159–177. https://doi.org/10.1007/s10236-013-0679-0
Naish T, Levy RH, Hamling IJ, Garner G, Hreinsdóttir S, Kopp RE, Golledge NR, Bell R, Paulik R, Lawrence J, and et al (2022) The significance of vertical land movements at convergent plate boundaries in probabilistic sea-level projections for AR6 scenarios: The new zealand case. Earth and Space Science Open Archive, page 33
Needham HF, Keim BD, Sathiaraj D (2015) A review of tropical cyclone-generated storm surges: global data sources, observations, and impacts. Rev Geophys (1985) 53(2):545–591. https://doi.org/10.1002/2014RG000477
Nerem RS, Chambers DP, Choe C, Mitchum GT (2010) Estimating mean sea level change from the TOPEX and Jason altimeter missions. Mar Geod 33:435–446
Nerem RS, Beckley BD, Fasullo JT, Hamlington BD, Masters D, Mitchum GT (2018) Climate-change–driven accelerated sea-level rise detected in the altimeter era. Proc Natl Acad Sci U S A 115:2022–2025. https://doi.org/10.1073/pnas.1717312115
Nguyen NM, Marchesiello P, Lyard F, Ouillon S, Cambon G, Allain D, Dinh VU (2014) Tidal characteristics of the gulf of Tonkin. Cont Shelf Res 91:37–56. https://doi.org/10.1016/j.csr.2014.08.003
Nguyen-Duy T, Ayoub NK, De Mey-Frémaux P, Ngo-Duc T (2023) How sensitive is a simulated river plume to uncertainties in wind forcing? A case study for the Red River plume (Vietnam). Ocean Modelling, https://doi.org/10.1016/j.ocemod.2023.102256
Nicholls RJ (2011) Planning for the impacts of sea level rise. Oceanography 24(2):144–157. https://doi.org/10.5670/oceanog.2011.34
Nicholls RJ, Lincke D, Hinkel J et al (2021) A global analysis of subsidence, relative sea-level change and coastal flood exposure. Nat Clim Chang 11:338–342. https://doi.org/10.1038/s41558-021-00993-z
Nurlatifah A et al (2021) Variability and trend of sea level in southern waters of Java, Indonesia, Journal of Southern Hemisphere, Earth. Syst Sci 71(3):272–283. https://doi.org/10.1071/ES21004
Oelsmann J, Passaro M, Sánchez L et al (2022) Bayesian modelling of piecewise trends and discontinuities to improve the estimation of coastal vertical land motion. J Geod 96:62. https://doi.org/10.1007/s00190-022-01645-6
Oelsmann J, Calafat FM, Passaro M, Hughes C, Richter K, Piecuch C et al (2024) Coherent modes of global coastal sea level variability. J Geophys Res Oceans 129:e2024JC021120. https://doi.org/10.1029/2024JC021120
Oelsmann J, Nicholls RJ, Lincke D et al (2026) Subsidence more than doubles sea-level rise today along densely populated coasts. Nat Commun 17:4382. https://doi.org/10.1038/s41467-026-72293-z
Ohenhen LO, Shirzaei M, Ojha C et al (2024) Disappearing cities on US coasts. Nature 627:108–115. https://doi.org/10.1038/s41586-024-07038-3
Opel L, Schindelegger M, Ray RD (2024) A likely role for stratification in long-term changes of the global ocean tides. Commun Earth Environ 5:261. https://doi.org/10.1038/s43247-024-01432-5
PAGES (2016) Past interglacials working group of PAGES interglacials of the last 800,000 years. Rev Geophys 54:162–219
Palmer MD, Domingues CM, Slangen AB, Boeira DF (2021) An ensemble approach to quantify global mean sea-level rise over the 20th century from tide gauge reconstructions. Environ Res Lett 16(4):044043. https://doi.org/10.1088/1748-9326/abdaec
Passaro M, Cipollini P, Vignudelli S, Quartly GD, Snaith HM (2014) ALES: a multi-mission adaptive subwaveform retracker for coastal and open ocean altimetry. Remote Sens Environ 145:173–189. https://doi.org/10.1016/j.rse.2014.02.008
Passaro M, Nadzir ZA, Quartly GD (2018) Improving the precision of sea level data from satellite altimetry with high-frequency and regional sea state bias corrections. Remote Sens Environ 1(218):245–254. https://doi.org/10.1016/j.rse.2018.09.007
Peltier WR (2004) Global glacial isostasy and the surface of the ice-age Earth: the ICE-5G (VM2) model and GRACE. Annu Rev Earth Planet Sci 32:111–149. https://doi.org/10.1146/annurev.earth.32.082503.144359
Peng D, Hill EM, Meltzner AJ, Switzer AD (2019) Tide gauge records show that the 18.61-year nodal tidal cycle can change high water levels by up to 30 cm. J Geophys Res 124:736–749. https://doi.org/10.1029/2018JC014695

Peng FK, Deng XL, Jiang MF, Dinardo S, Shen YZ (2023) A new method to combine coastal sea surface height estimates from multiple retrackers by using the Dijkstra algorithm. Remote Sens 15:2329. https://doi.org/10.3390/rs15092329

Peng F, Deng X, Shen Y, Cheng X (2025) The International Altimetry Service 2024 (IAS2024) coastal sea level dataset and first evaluations. Earth Syst Sci Data 17:1441–1460. https://doi.org/10.5194/essd-17-1441-2025

Pham NT, Staneva J, Bonaduce A et al (2024) Interannual sea level variability in the North and Baltic seas and net flux through the Danish straits. Ocean Dyn 74:669–684. https://doi.org/10.1007/s10236-024-01626-7

Piecuch CG (2023) River effects on sea-level rise in the Río de la Plata estuary during the past century. Ocean Sci 19:57–75. https://doi.org/10.5194/os-19-57-2023

Piecuch CG, Bittermann K, Kemp AC, Ponte RM, Little CM, Engelhart SE, Lentz SJ (2018) River-discharge effects on United States Atlantic and Gulf coast sea-level changes. Proc Natl Acad Sci U S A 115:7729–7734. https://doi.org/10.1073/pnas.1805428115

Pineau-Guillou L, Bouin MN, Ardhuin F, Lyard F, Bidlot JR, Chapron B (2020) Impact of wave-dependent stress on storm surge simulations in the North Sea: ocean model evaluation against in situ and satellite observations. Ocean Model. https://doi.org/10.1016/j.ocemod.2020.101694

Pineau-Guillou L, Lazure P, Wöppelmann G (2021) Large-scale changes of the semidiurnal tide along North Atlantic coasts from 1846 to 2018. Ocean Sci 17:17–34. https://doi.org/10.5194/os-17-17-2021

Piton V, Herrmann M, Lyard F, Marsaleix P, Duhaut T, Allain D, Ouillon S (2020) Sensitivity study on the main tidal constituents of the Gulf of Tonkin by using the frequency-domain tidal solver in T-UGOm. Geosci Model Dev 13:1583–1607. https://doi.org/10.5194/gmd-13-1583-2020

Ponte RM et al (2019) Towards comprehensive observing and modeling systems for monitoring and predicting regional to coastal sea level. Front Mar Sci 6:437. https://doi.org/10.3389/fmars.2019.00437

Prandi P, Meyssignac B, Ablain M et al (2021) Local sea level trends, accelerations and uncertainties over 1993–2019. Nat Sci Data 626(8):1. https://doi.org/10.1038/s41597-020-00786-7

Preisendorfer RW (1988) Principal Component Analysis in Meteorology and Oceanography Mobley CD, 425, Elsevier Science, New York

Pugh DT, and Woodworth PL (2014) Sea-level science: understanding tides, surges, tsunamis and mean sea-level changes. Cambridge: Cambridge University Press. 395pages, ISBN 978-1-107-02819-7

Qu T, Fukumori I, Fine RA (2019) Spin-up of the Southern Hemisphere super gyre. J Geophys Res Oceans 124:154–170. https://doi.org/10.1029/2018JC014391

Qu Y, Jevrejeva S, Palanisamy H (2023) Are near-coastal sea levels accelerating faster than global during the satellite altimetry era? Atmosphere (Basel). https://doi.org/10.3390/atmos14101573

Rasquin C, Seiffert R, Wachler B, Winkel N (2020) The significance of coastal bathymetry representation for modelling the tidal response to mean sea level rise in the German Bight. Ocean Sci 16(1):31–44

Ray RD (2022) Technical note: on seasonal variability of the M_2 tide. Ocean Sci 18:1073–1079. https://doi.org/10.5194/os-18-1073-2022

Ray RD, Merrifield MA (2019) The semiannual and 4.4-year modulations of extreme high tides. J Geophys Res Oceans 124:5907–5922. https://doi.org/10.1029/2019JC015061

Riser SC, Freeland HJ, Roemmich D, Wijffels S, Troisi A, Belbéoch M et al (2016) Fifteen years of ocean observations with the global Argo array. Nat Clim Change 6:145–153. https://doi.org/10.1038/nclimate2872

Rodriguez ED Esteban Fernandez E, Peral CW, Chen J-W De Bleser, Williams B (2017) Wide-swath altimetry: a review. In: "Satellite altimetry over oceans and land surfaces", Book Chapter 2. Eds D. Stammer & A. Cazenave, CRC Press, Taylor and Francis Group, Boca Raton, New York, London, ISBN: 13: 978–1–4987–4345–7

Roelvink D, Reniers A, van Dongeren A, de Vries JVT, McCall R, Lescinski J (2009) Modeling storm impacts on beaches, dunes and barrier islands. Coast Eng 56(11–12):1133–1152. https://doi.org/10.1016/j.coastaleng.2009.08.006

Rohling EJ, Foster GL, Gernon TM et al (2022) Comparison and synthesis of sea-level and deep-sea temperature variations over the past 40 million years. Rev Geophys 60(4):e2022RG000775. https://doi.org/10.1029/2022RG000775

Rong Y, Bates P, Neal J, Bell P, Gommenginger C, Lichtman ID et al (2026) Evaluating SWOT in the coastal zone: comparisons with tide gauge and airborne LiDAR in the Bristol Channel and Severn Estuary, UK. Geophys Res Lett 53:e2025GL116590. https://doi.org/10.1029/2025GL116590

Rose L, Widlansky MJ, Feng X, Thompson P, Asher TG, Dusek G, Blanton B, Luettich RA Jr, Callahan J, Brooks W, Keeney A, Haddad J, Sweet W, Genz A, Hovenga P, Marra J, Tilson J (2024) Assessment of water levels from 43 years of NOAA's Coastal Ocean Reanalysis (CORA) for the Gulf of Mexico and East Coasts. Front Mar Sci 11:1381228. https://doi.org/10.3389/fmars.2024.1381228

Royston S, Vishwakarma BD, Westaway RM, Rougier J, Sha Z, and Bamber JL (2020) Can we resolve the basin-scale sea level 557 trend budget from GRACE ocean mass? JGeophys Res- Oceans, 125, e2019JC015535. 558, https://doi.org/10.1029/2019JC015535

Saemian P, Elmi O, Stroud M, Riggs R, Kitambo BM, Papa F, Allen GH, Tourian MJ (2025) Satellite altimetry-based extension of global-scale in situ river discharge Measurements (SAEM). Earth Syst Sci Data 17:2063–2085. https://doi.org/10.5194/essd-17-2063-2025

Saha S et al (2010) The NCEP climate forecast system reanalysis. Bull Am Meteorol Soc 91:1015–1057. https://doi.org/10.1175/2010BAMS3001.1

Salameh E, Desroches D, Deloffre J, Fjørtoft R, Mendoza ET, Turki I, Froideval L, Levaillant R, Déchamps S, Picot N, Laignel B, Frappart F (2024) Evaluating SWOT's interferometric capabilities for mapping intertidal topography. Remote Sens Environ 314:114401. https://doi.org/10.1016/j.rse.2024.114401

Sánchez L, Bosch W (2009) The role of the TIGA project in the unification of classical height systems. In: Drewes H (ed) Geodetic reference frames, IAG symposia 134. Springer, pp 285–290. https://doi.org/10.1007/978-3-642-00860-3

Sanchez-Roman A, Jorda G, Sannino G, Gomis D (2018) Modelling study of transformations of the exchange flows along the strait of Gibraltar. Ocean Sci 14(6):1547–1566. https://doi.org/10.5194/os-14-1547-2018

Sanli DU, Blewitt G (2001) Geocentric sea level trend using GPS and >100-year tide gauge record on a postglacial rebound nodal line. J Geophys Res 106(B1):713–719. https://doi.org/10.1029/2000JB900348

Santamaría-Gómez A, Gravelle M, Collilieux X, Guichard M, Míguez BM, Tiphaneau P, Wöppelmann G (2012) Mitigating the effects of vertical land motion in tide gauge records using a state-of-the-art GPS velocity field. Global Planet Change 98–99:6–17. https://doi.org/10.1016/j.gloplacha.2012.07.007

Save H, Bettadpur S, Tapley BD (2016) High-resolution CSR GRACE RL05 mascons. J Geophys Res Solid Earth 121:7547–7569. https://doi.org/10.1002/2016JB013007

Schossler V, Aquino FE, Simões JC, Silva RC, Hofmann GS, Vianna DR, Lira PHR, Pozzi G, Oliveira AM (2024) Role of the Southern Annular Mode in the sea level over the southern Blue Amazon. An Acad Bras Cienc 16(96):e20240592. https://doi.org/10.1590/0001-3765202420240592

Seeger K, Minderhoud PSJ (2026) Sea level much higher than assumed in most coastal hazard assessments. Nature 652:667–674. https://doi.org/10.1038/s41586-026-10196-1

Seifi F, Filmer M (2023) Residual M2 and S2 ocean tide signals in complex coastal zones identified by X-Track reprocessed altimetry data. Continental Shelf Res. https://doi.org/10.1016/j.csr.2023.105013

Shirzaei M, Freymueller J, Törnqvist TE, Galloway DL, Dura T, Minderhoud PSJ (2021) Measuring, modelling and projecting coastal land subsidence. Nature Rev Earth Environ 2(1):40–58. https://doi.org/10.1038/s43017-020-00115-x

Siddorn JR, Furner R (2013) An analytical stretching function that combines the best attributes of geopotential and terrain-following vertical coordinates. Ocean Model. https://doi.org/10.1016/j.ocemod.2013.02.001

Simon B (2007) La marée océanique côtière, Collection Synthèses Institut Océanographique Paris 978-2-903581-32-9. 433 pp

Spada G (2017) Glacial isostatic adjustment and contemporary sea level rise: an overview. Surv Geophys 38:153–185

Sprintall J et al (2019) Detecting change in the Indonesian seas. Front Mar Sci 6:257. https://doi.org/10.3389/fmars.2019.00257

Stammer D, Cazenave A (2018) Applications of satellite altimetry over oceans and land surfaces CRC Press Taylor & Francis 978-1-4987-4345-7, 690 pages

Stockdon HF, Holman RA, Howd PA, Sallenger AH (2006a) Empirical parameterization of setup, swash, and runup. Coast Eng 53:573–588

Stockdon HF, Holman RA, Howd PA, Sallenger AH (2006b) Empirical parameterization of setup, swash, and runup. Coast Eng 53:573–588. https://doi.org/10.1016/j.coastaleng.2005.12.005

Sturges W, Leben R (2000) Frequency of ring separations from the loop current in the Gulf of Mexico : a revised estimate. J Phys Oceanogr 30(7):1814–1819. https://doi.org/10.1175/1520-0485

Sun J, Zhang L, Hu D (2022a) Decadal and long-term variability of sea level in the Southwestern Pacific during 1948–2018. Geophys Res Lett 49:e2022GL098747. https://doi.org/10.1029/2022GL098747

Sun J, Zhang L, Hu D (2022) Decadal and long-term variability of sea level in the Southwestern Pacific during 1948–2018. Geophys Res Lett 49, e2022GL098747

SWAN Group (2024), SWAN User Manual—SWAN Cycle III version 41.45, Delft University of Technology, Delft, Netherlands

Sweet W, Hamlington B, Kopp RE, Weaver C, Barnard PL, Bekaert D, Brooks W, Craghan M, Dusek G, Frederikse T, Garner G, Genz AS, Krasting JP, Larour E, Marcy D, Marra JJ, Obeysekera J, Osler M, Pendleton M, Roman D, Schmied L, Veatch W, White K, and Zuzak C, (2022) Global and regional sea level rise scenarios for the United States: Technical Report NOS.01, xiv, 95 p

Talke SA, Jay DA (2020) Changing tides: the role of natural and anthropogenic factors. Annu Rev Mar Sci 12:121–151. https://doi.org/10.1146/annurev-marine-010419-010727

Tamisiea ME (2011) Ongoing glacial isostatic contributions to observations of sea level change. Geophys J Int 186:1036–1044. https://doi.org/10.1111/j.1365-246X.2011.05116.x

Tapley BD, Bettadpur S, Watkins M, Reigber C (2004) The Gravity Recovery and Climate Experiment: mission overview and early results. Geophys Res Lett 31:2004GL019920. https://doi.org/10.1029/2004GL019920

Tapley B, Watkins MM, Flechtner F, Reigber C et al (2019) Contributions of GRACE to understanding climate change. Nat Clim Change 9:358–369. https://doi.org/10.1038/s41558-019-0456-2

Taveneau A, Almar R, Bergsma EW, Sy BA, Ndour A, Sadio M, Garlan T (2021) Observing and predicting coastal erosion at the Langue de Barbarie sand spit around Saint Louis (Senegal, West Africa) through satellite-derived digital elevation model and shoreline. Remote Sens 13(13):2454

The WAVEWATCH III Development Group. User manual and system documentation of WAVEWATCH III version 5.16. NOAA / NWS / NCEP / MMAB Technical Note 329, 2016; 326 pp

Thiéblemont R, Le Cozannet G, Nicholls RJ, Rohmer J, Wöppelmann G, Raucoules D et al (2024) Assessing current coastal subsidence at continental scale: insights from Europe using the European Ground Motion Service. Earths Future 12:e2024EF004523. https://doi.org/10.1029/2024EF004523

Törnqvist TE, Blum MD (2024) What is coastal subsidence? Cambridge Prisms: Coastal Futures. 2:e2. https://doi.org/10.1017/cft.2024.1

Uchiyama Y, McWilliams JC, Restrepo JM (2009) Wave-current interaction in nearshore shear instability analyzed with a vortex force formalism. J Geophys Res 114:C06021. https://doi.org/10.1029/2008JC005135

Uchiyama Y, McWilliams JC, Shchepetkin AF (2010) Wave–current interaction in an oceanic circulation model with a vortex-force formalism: application to the surf zone. Ocean Model 34:16–35. https://doi.org/10.1016/j.ocemod.2010.04.002

Uchiyama Y, McWilliams JC, Akan C (2017) Three-dimensional transient rip currents: bathymetric excitation of low-frequency intrinsic variability. J Geophys Res Oceans 122:5826–5849. https://doi.org/10.1002/2017JC013005

Van Veen J (1945) Bestaat er een geologische bodemdaling te Amsterdam sedert 1700? Tijdschr K Ned Aardrijksk Genoot LXII, 2–36

Vignudelli S et al (2019) Satellite altimetry measurements of sea level in the coastal zone. Surv Geophys. https://doi.org/10.1007/s10712-019-09569-1

Vitousek S, Barnard PL, Fletcher CH, Frazer N, Erikson L, Storlazzi CD (2017) Doubling of coastal flooding frequency within decades due to sea-level rise. Sci Rep 7:1399. https://doi.org/10.1038/s41598-017-01362-7

Volkov DL, Zhang K, Johns W, Willis J, Hobbs W, Goes M, Zhang H, Menemenlis D (2023) Atlantic meridional overturning circulation increases flood risk along the United States southeast coast. Nat Commun 14:5095. https://doi.org/10.1038/s41467-023-40848-z

Vos K, Harley MD, Splinter KD, Walker A, Turner IL (2020) Beach slopes from satellite‐derived shorelines. Geophys Res Lett 47(14):e2020GL088365

Vousdoukas MI, Mentaschi L, Voukouvalas E, Verlaan M, Jevrejeva S, Jackson LP, Feyen L (2018) Global probabilistic projections of extreme sea levels show intensification of coastal food hazard. Nat Commun 9:2360. https://doi.org/10.1038/s41467-018-04692-w

Wahl T, Chambers DP (2015) Evidence for multidecadal variability in US extreme sea level records. J Geophys Res Oceans 120(3):1527–1544

WAMDI Group (1988) The WAM model—a third generation ocean wave prediction model. J Phys Oceanogr 18:1775–1810

Wang P, Bernier NB (2025) Advancing global hindcast of extreme sea levels: insights from a 65-year study. Weather Clim Extremes. https://doi.org/10.1016/j.wace.2025.100805

Wang H, Liu K, Gao Z, Fan W, Liu S, Li J (2017) Characteristics and possible causes of the seasonal sea level anomaly along the South China Sea coast. Acta Oceanol Sin 36:9–16. https://doi.org/10.1007/s13131-017-0988-0

Wang J, Yi S, Li M, Wang L, Song C (2018) Effects of sea level rise, land subsidence, bathymetric change and typhoon tracks on storm flooding in the coastal areas of Shanghai. Sci Total Environ 621:228–234

Wang J, Church JA, Zhang X, Gregory JM, Zanna L, Chen X (2021) Evaluation of the local sea-level budget at tide gauges since 1958. Geophys Res Lett 48:e2021GL094502. https://doi.org/10.1029/2021GL094502
Watkins MM, Wiese DN, Yuan D-N, Boening C, Landerer FW (2015) Improved methods for observing Earth's time variable mass distribution with GRACE using spherical cap mascons. J Geophys Res Solid Earth 120:2648–2671. https://doi.org/10.1002/2014JB011547
WAVEWATCH III Development Group (WW3DG)(2016) Published version 5.16 of the WAVEWATCH III user manual and systemdocumentation in October 2016 (Technical Note 329 by NOAA/NWS/NCEP/MMAB)
WCRP Global Sea Level Budget Group (The) (2018) Global sea level budget, 1993-present. Earth Syst Sci Data 10:1551–1590. https://doi.org/10.5194/essd-10-1551-2018
Weiss L, Estournel C, Marsaleix P, Mikolajczak G, Constant M, Ludwig W (2024) From source to sink: part 1—characterization and Lagrangian tracking of riverine microplastics in the Mediterranean Basin. Environ Sci Pollut Res. https://doi.org/10.1007/s11356-024-34635-6
Weiss L, Herrmann M, Marsaleix P, Bompoil M, and Maes C (2025) Modeling Indian Ocean circulation to study marine debris dispersion: insights into high-resolution and Stokes drift effects with Symphonie 3.6.6, EGUsphere [preprint], https://doi.org/10.5194/egusphere-2025-1918
Whitehouse PL (2018) Glacial isostatic adjustment modelling: historical perspectives, recent advances, and future directions. Earth Surf Dyn 6:401–429. https://doi.org/10.5194/esurf-6-401-2018
Wiese DN, Landerer FW, Watkins MM (2016) Quantifying and reducing leakage errors in the JPL RL05M GRACE mascon solution. Water Resour Res 52:7490–7502. https://doi.org/10.1002/2016WR019344
Woodworth PL et al (2019) Forcing factors affecting sea level changes at the coast. Surv Geophys 40:1351–1397. https://doi.org/10.1007/s10712-019-09531-1
Wöppelmann G, Marcos M (2016) Vertical land motion as a key to understanding sea level change and variability. Rev Geophys 54:64–92. https://doi.org/10.1002/2015RG000502
Wöppelmann G, Martin Miguez B, Bouin M-N, Altamimi Z (2007) Geocentric sea-level trend estimates from GPS analyses at relevant tide gauges world-wide. Glob Planet Change 57:396–406. https://doi.org/10.1016/j.gloplacha.2007.02.002
Wright LD, Short AD (1984a) Morphodynamic variability of surf zones and beaches: a synthesis. Mar Geol 56(1–4):93–118
Wright LD, Short AD (1984b) Morphodynamic variability of surf zones and beaches: a synthesis. Mar Geol 56(1–4):93–118. https://doi.org/10.1016/0025-3227(84)90008-2
Xu Z, Bowen AJ (1994) Wave- and wind-driven flow in water of finite depth. J Phys Oceanogr 24:1850–1866. https://doi.org/10.1175/1520-0485
Zhang X, Han W (2020) Effects of climate modes on interannual variability of upwelling in the tropical Indian Ocean. J Clim 33:1547–1573. https://doi.org/10.1175/JCLI-D-19-0386.1
Zhang L, Delworth TL, Koul V, Ross A, Stock C, Yang X, Zeng F, Wittenberg A, Zhao J, Gu Q, Li S (2025) Skillful multiyear prediction of flood frequency along the US Northeast Coast using a high-resolution modeling system. Sci Adv 11:20. https://doi.org/10.1126/sciadv.ads4419
Zhu Y, Han W, Alexander MA, Shin SI (2024) Interannual sea level Variability along the US east coast during the satellite altimetry era: local versus remote forcing. J Climate 37(1):21–39. https://doi.org/10.1175/JCLI-D-23-0065.1
Zhu Y, Han W, Alexander M, (2023) Nonstationary Roles of Regional Forcings in Driving Low-frequency Sea level Variability Along the U.S. East Coast since the 1950s. Geophys Res Lett https://doi.org/10.1029/2023GL104191
Zijlema M, Stelling GS, Smit PB (2011) SWASH: an operational public-domain code for simulating wave fields and rapidly varied flows in coastal waters. Coast Eng 58(10):992–1012. https://doi.org/10.1016/j.coastaleng.2011.05.015
Zuo H, Balmaseda MA, Tietsche S, Mogensen K, Mayer M (2019) The ECMWF operational ensemble reanalysis-analysis system for ocean and sea ice: a description of the system and assessment. Ocean Sci 15:779–808. https://doi.org/10.5194/os-15-779-2019

Authors and Affiliations

A. Cazenave[1] · R. Almar[1] · P. Almeida[2] · N. K. Ayoub[1] · J. H. Bettencourt[3] · F. Birol[1] · W. Han[4] · M. Herrmann[1] · S. Jevrejeva[5] · L. Leclercq[1] · F. Niño[1] · J. Oelsmann[6] · F. Papa[1] · S. Ponce de León[7,8] · A. Tarpanelli[9] · V. D. Vinh[10]

✉ A. Cazenave
anny.cazenave@gmail.com

1 LEGOS (CNES/CNRS/IRD/UT), Université de Toulouse, Toulouse, France

2 Instituto Dom Luiz (IDL), Faculdade de Ciências, Universidade de Lisboa, Campo Grande, Lisbon, Portugal

3 Stockholm Environment Institute, Stockholm, Sweden

4 University of Colorado, Boulder, USA

5 National Oceanography Centre, Liverpool, UK

6 Department of River-Coastal Science and Engineering, Tulane University, New Orleans, USA

7 Institute of Marine Science (ICM), Spanish Research Council (CSIC), Institut de Recerca Per a La Governança del Mar (ICATMAR), Barcelona, Spain

8 Centre for Marine Technology and Ocean Engineering (CENTEC), Instituto Superior Técnico, Universidadede Lisboa, Lisbon, Portugal

9 National Research Council, Research Institute for Geo-Hydrological Protection, Perugia, Italy

10 Institute of Oceanography, Vietnam Academy of Science and Technology (VAST), Hanoi, Vietnam